Reviews

Strain-induced fibrillation of glassy polymers

A. L. Volynskii,[a] E. G. Rukhlya,[a] A. Yu. Yarysheva,[a] O. V. Arzhakova,[a] A. S. Kechek´yan,[b] L. M. Yarysheva,[a] P. A. Kechek´yan,[a] and A. A. Dolgova[a]*

[a] *Department of Chemistry, M. V. Lomonosov Moscow State University, Build. 3, 1 Leninskie Gory, 119991 Moscow, Russian Federation. Fax: +7 (495) 939 0174. E-mail: katrin310@yandex.ru*
[b] *N. S. Enikolopov Institute of Synthetic Polymeric Materials, Russian Academy of Sciences, 70 ul. Profsoyuznaya, 117393 Moscow, Russian Federation. Fax: +7 (495) 718 3404*

Literature data on structural rearrangements taking place in amorphous glassy polymers upon their plastic deformation are analyzed. This deformation is shown to be primarily accompanied by polymer self-dispersion into fibrillar aggregates composed of oriented macromolecules with a diameter of 1—10 nm. The above structural rearrangements proceed independently of the deformation mode of polymers (cold drawing, crazing, or shear banding of polymers under the conditions of uniaxial drawing or uniaxial compression). Principal characteristics of the formed fibrils and the conditions providing their development are considered. Information on the properties of the fibrillated glassy polymers is presented, and the pathways of their possible practical application are highlighted.

Key words: fibrillation, self-dispersion, free volume, hydrostatic pressure, thermal aging, mechanical and thermomechanical properties of fibrillated polymers.

Introduction

Fibrillation or, in other words, the ability of macromolecules to produce highly asymmetric fibrous aggregates is known to be an intrinsic property of polymers. These aggregates can be either spontaneously developed in polymer solutions[1,2] or can be formed directly in the course of polymerization.[3] Figure 1 presents the electron micrograph of the sample of the rigid-chain polymer, poly-γ-benzyl-L-glutamate, prepared by evaporation from the solution.[2]

As follows from Fig. 1, upon precipitation of this polymer from the solution, formation of asymmetric fibrous aggregates with well-pronounced fibrillar morphology takes place. The development of fibrillar aggregates is also observed for natural fibers, for example, for different types of cellulose and its derivatives,[4—6] collagen,[7,8] *etc*. The above types of fibrillation are provided by the specific character of phase separation taking place in the solutions of rigid-chain polymers or by the specific features of biosynthesis in natural objects, but this particular topic is

Published in Russian in *Izvestiya Akademii Nauk. Seriya Khimicheskaya,* No. 1, pp. 0001—0022, January, 2018.
1066-5285/18/6701-0001

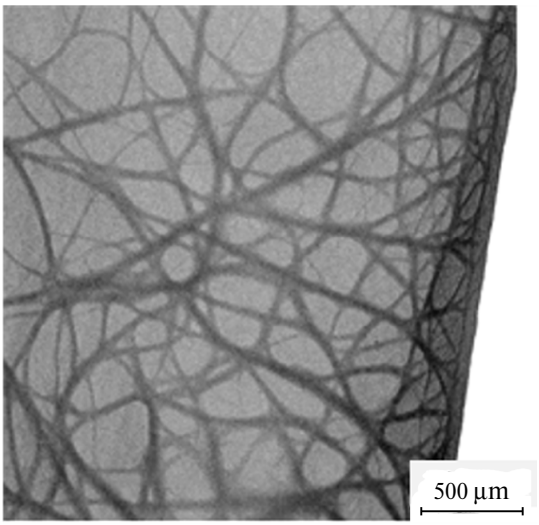

Fig. 1. Electron micrograph of the sample of poly-γ-benzyl-L-glutamate prepared by evaporation from the solution.[22]

beyond the scope of our review. The present review addresses the universal phenomenon of fibrillation primarily for amorphous glassy polymers upon their plastic deformation.

Conditions providing the development of a fibrillar structure upon deformation of glassy polymers

Noteworthy is that the ability of glassy polymers to produce fibrils is most pronounced upon their cold drawing. Figure 2 shows the electron microscopic image of thin (~0.5 μm) polystyrene (PS) films after their uniaxial stretching at room temperature.[9] Thin (nanoscale) PS films and fibers[10] are able to experience marked plastic deformation via necking, even though PS is known to be a brittle polymer at ambient temperatures. As follows from Fig. 2, tensile drawing of the polymer sample is accompanied by the formation of a local region of a plastically deformed material (a neck) composed of fibrillar aggregates with a diameter of 20—50 nm, and these aggregates are oriented along the direction of the applied force.

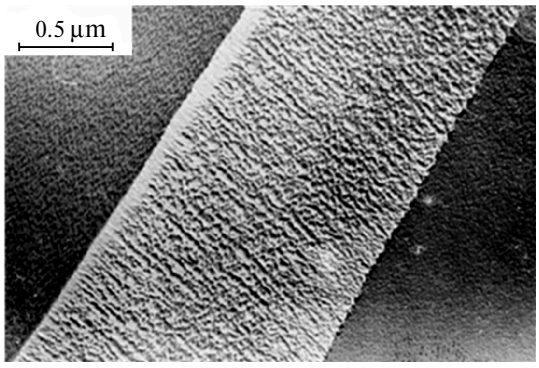

Fig. 2. Electron micrograph of the thin PS film after deformation.[9] The direction of tensile drawing is horizontal.

Let us consider the specific features of the fibrillar structure in polymers produced upon their cold drawing. This structure features the assay of densely packed fibrillar elements with a diameter ranging from several to tens of nanometers. Despite their dense packing, fibrils have well-pronounced interfacial boundaries, and their existence has been convincingly proved by the electron microscopy[11,12] and X-ray analysis.[13] Mechanical properties of the oriented polymer are primarily controlled by the existence of real physical boundaries between the fibrils. According to the present knowledge, the principal resistance to deformation of the oriented polymer is provided by quasi-elastic friction forces acting on the highly developed surface of sliding fibrils.[14] Abundant experimental evidence on fibrillar morphology and diverse fibers based on natural and synthetic polymers has been reported in the review;[11] and the fibrillar structure appears to be universal for virtually all oriented polymer systems. In this structure, the diameter of individual fibrils falls within the range from several to tens nanometers.

Molecular orientation of the amorphous polymer can be achieved via two different ways: first, via uniform stretching of a polymer in a rubbery state and its further cooling and stabilization of the attained orientation; second, via stretching a glassy polymer (so-called cold or orientational drawing). According to the results of numerous studies, fibrillation of polymers is found to be the consequence of orientational drawing[15].

Crucial importance of the orientation mode is also related to the fact that polymers oriented in the above two ways are characterized by different morphology and some characteristics. Noteworthy is that fibrillation of polymers seems to be interesting not only from the academic viewpoint. This process has been widely used since long ago.[16] For example, according to the general knowledge, under the external mechanical impact, highly oriented polymer films are disintegrated into fibers along the boundaries of the existing fibrils (so-called film filaments), which are used for the preparation of synthetic felt or yarn for the fabrication of textiles. This approach can be applied to polyolefins, cellulose derivatives, polyesters, poly(vinyl chloride).

The problem concerning the development of interfacial (interfibrillar) boundaries in the initial monolithic glassy polymer is closely related to the two following structural aspects: 1) evolution of free volume upon deformation of the polymer, 2) molecular mobility in the glassy polymer and its correlation with the applied mechanical impact. Evidently, both factors control the development of interfacial boundaries in the deformed polymer. Formation of fibrillar macromolecular aggregates requires the fulfillment of the following conditions. First, this process requires a certain space, where macromolecules

(or their fragments) can move, change their conformations, and produce oriented macromolecular aggregates (fibrils). Second, the formation of fibrils in the unoriented glassy polymer necessitates sufficiently high molecular mobility of polymer chains. This molecular mobility is induced by the applied mechanical stress and provides the interaction, which assists the development of the fibrillar structure in polymers. Let us consider in detail the effect of both factors on the stress-induced development of fibrils in glassy polymers.

Volume effects of plastic deformation of glassy polymers

Cold drawing of polymers is known to be accompanied by the mutual orientation of macromolecular chains and by the development of fibrillar structural elements with well-pronounced interfacial boundaries. At the same time, existing concepts concerning cold drawing of glassy polymers ignore the description of this process.[17—22] In the analysis of the fibrillation mechanism of polymers upon their plastic deformation, the key point is concerned with the development of interfacial boundaries in the initially uniform and monolithic polymer.

Evidently, the development of interfacial boundaries in the polymer requires the formation of a certain excessive volume upon deformation, which accommodates the above structural rearrangements. In this connection, of special importance is the volume evolution upon deformation of polymer glasses. The initial glassy polymer is a system of randomly entangled macromolecules with a certain fraction of free volume, which, in turn, depends on temperature and polymer prehistory.[23] The development of interfacial (interfibrillar) boundaries upon cold drawing of glassy polymers is genetically related not only to the mutual orientation of macromolecules but also to the free volume evolution in the course of deformation. Evidently, the above development of interfacial boundaries in the initially monolithic polymer is not allowed without changes in the overall volume of the polymer sample because, in this case, a certain space is required for the further structural rearrangements. In particular, these speculations are supported by the data on direct measurements of the volume of the polymer samples in the course of their deformation. In contrast to rubbery polymers which preserve their volume upon deformation,[24] in glassy polymers, these phenomena are well pronounced. Figure 3 shows the stress—strain curve of poly(ethylene terephthalate) (PET) in comparison with the directly measured volume changes.[25]

Noteworthy is that the above phenomenon of the volume growth is observed not only under the conditions of uniaxial stretching but also upon uniaxial compression. Figure 4 presents the stress—strain curves and stress relaxation curves of poly(vinyl formal) in comparison with the concomitant changes in the volume of the polymer

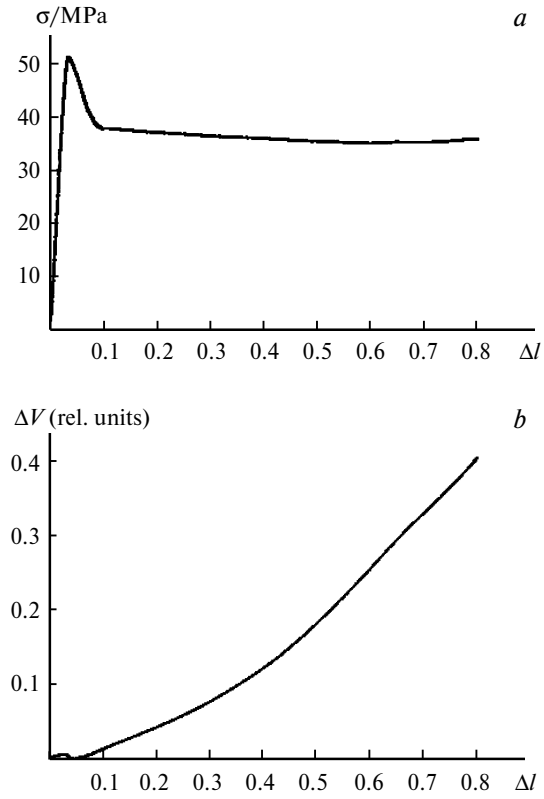

Fig. 3. Stress—strain curve of PET at room temperature (*a*) and the concomitant changes in the volume of the polymer sample upon deformation (*b*)[25] (σ is the true stress, Δl is the true strain, ΔV is the volume strain).

sample under uniaxial compression.[26] As follows from Fig. 4, under the above conditions, stress loading of the polymer sample is also accompanied by marked volume changes (volume growth). Moreover, the data presented in Fig. 4 illustrate another specific feature of the above volume changes. When uniaxial compression is ceased and stress relaxation takes place, overall volume of the polymer sample decreases. This evidence unequivocally highlights high structural lability of the deformed polymer, and the details of this phenomenon will be discussed below.

Even though the phenomenon of the overall volume changes is well-pronounced (see Fig. 3), detailed analysis of the free volume evolution provides the important information on the structural rearrangements taking place upon deformation of polymers. One of the most resourceful methods is the method of positron annihilation lifetime spectroscopy (PALS).[27—36]

The basic principle of the PALS method can be described as follows. A positron being introduced into a polymer annihilates with the environment. Prior to this annihilation, it exists as a free positron (lifetime ~0.3—0.5 ns) or as an orthopositronium (o-Ps) in the bound state. Usually, o-Ps is entrapped within microvoids, which serve as certain free volume holes and can be

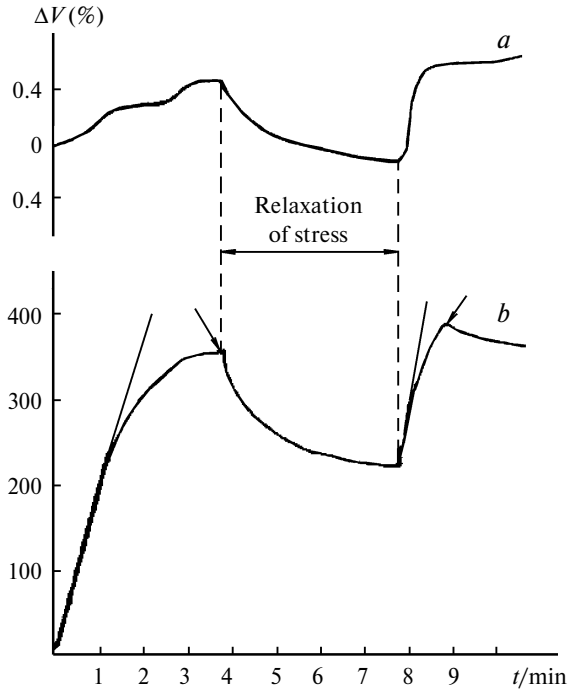

Fig. 4. Volume changes (ΔV) (*a*) and the stress—strain curve (σ is the stress) under uniaxial compression (*b*) for poly(vinyl formal) at room temperature. Arrows show the strains whereas tensile drawing is stopped[26] (within the temperature interval from 0 to 4 min the sample was loaded; the, the stress was released).

detected by the PALS spectra. The lifetime of o-Ps is reduced down to several nanoseconds when the positron annihilates with the electron from the surrounding molecules. Therefore, the lifetime of o-Ps (τ_3) in the sample is the factor that is controlled by void dimensions at the microscale level (~5—10 E); at the same time, the annihilation irradiation intensity is unusually assumed to be proportional to the probability of the o-Ps formation and, hence, to the density of free volume holes. The parameter τ_3 is provided by the o-Ps annihilation upon the entrapment within the free volume holes and is known to be sensitive to temperature variations and mechanical loading.[37] The τ_3 value is found to depend on the radius of microvoids, where Ps is localized.[28,38] The intensity of positron annihilation process (I_3) is also controlled by temperature changes and by loading. Usually, this parameter is related to the density (number) of free volume holes, and this observation allows the assessment of the overall volume of holes (ΔV_h), where o-Ps is localized under the different impacts on the polymer sample.

Figure 5 highlights the advantages of the PALS method for the studies of thermal expansion of the amorphous polymer.[37] Noteworthy is that, during several recent decades, thermal expansion of polymeric glasses has been studied in detail;[39—42] the results of these studies were interpreted in terms of various models. Thermal expansion of the materials as a simple structural change can be easily studied because any material can experience it without any external mechanical or chemical impact. Glassy polymers are able to experience several temperature-dependent structural transitions. Of primary importance is the temperature interval of glass transition, where the degree of freedom of molecular chains and their mobility are markedly changed.

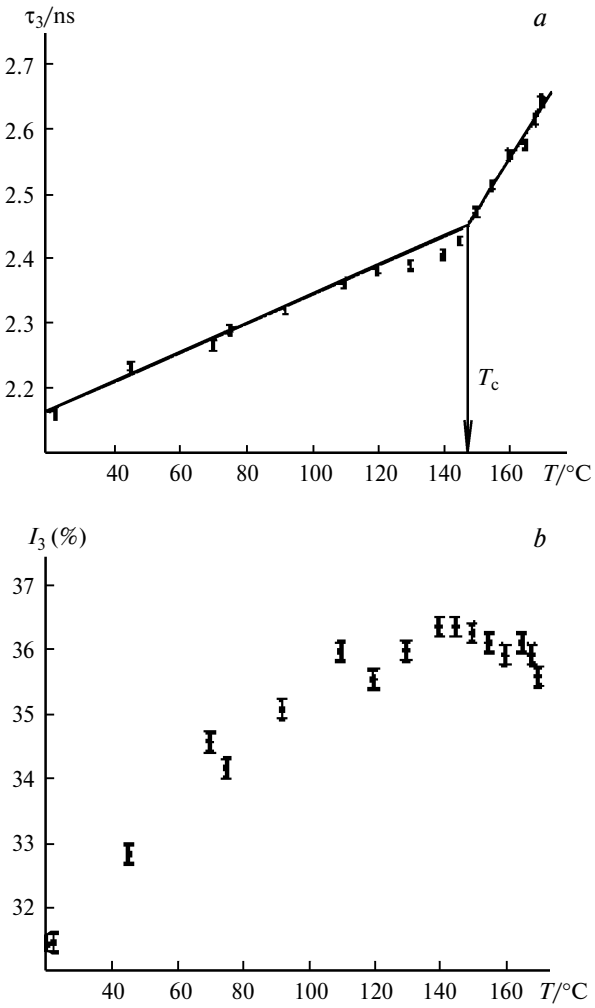

Fig. 5. The temperature dependence of parameters τ_3 (*a*) and I_3 (*b*) for PC.[37]

As follows from Fig. 5, when the polymer sample is heated within the temperature interval of 25—170 °C, the radius of free volume holes increases from 0.293 to 0.332 nm. The inclined region in Fig. 5, *a* corresponds to the glass transition temperature of the polymer. The number of holes characterized by the parameter I_3 also increases with increasing temperature to 110 °C; then, this number reaches its saturation. Similar behavior was observed for other polymers.[39,43—45] The growth in the number of holes with increasing temperature suggests that the entrapment sites have the temperature-induced nature.

The plateau region in the corresponding plot is likely to be related to the attainment of the equilibrium concentration of the entrapment sites at the glass transition point.

Therefore, the PALS method is very sensitive to the free-volume evolution in glassy polymers upon thermal expansion with temperature. Moreover, this method can be also applied to polymers under mechanical loading under isothermic conditions. As was shown in numerous experiments, plastic deformation of glassy polymers is accompanied by a marked increase in their free volume. Noteworthy is that free volume starts to increase once the yield point is attained, and this behavior is observed not only under the conditions of uniaxial stretching and uniaxial compression.

Free volume of the polymer defines its glass transition temperature (T_g) because the segmental cooperative molecular motion requires the existence of a certain free space (free volume). In this connection, the external hydrostatic pressure strongly controls T_g (Fig. 6, *a*).[46] The higher the applied hydrostatic pressure (hydrostatic compression), the lower the free volume of the polymer; the sufficient level of free volume providing large-scale (segmental) molecular motion is attained at the higher temperature and at the higher stress. In other words, the higher the hydrostatic pressure applied to the polymer, the higher the glass transition temperature T_g, and this scenario is observed in the experiments (see Fig. 6, *a*).

Therefore, free volume controls not only the specific features of the molecular mobility of glassy polymers (in particular, glass transition temperature T_g can serve as its measure) but also the related key macroscopic characteristics of the polymer, including yield point and strength. Hence, the above characteristics also strongly depend on the applied hydrostatic pressure (see Fig. 6, *b*). Yield point of the polymer is the state where its orientational transformation takes place (commences). Orientation of polymers proceeds via the displacement of big-sized fragments of polymer chains (segments). Evidently, the development of these processes also requires the existence of the sufficient free volume fraction, which, in turn, depends on the applied hydrostatic pressure. Evidently, both yield point (see Fig. 6, *b*, curve *1*) and elongation at break (see Fig.6, *b*, curve *2*) are directly proportional to the hydrostatic pressure.

Numerous studies are devoted to the free volume evolution in the course of plastic deformation of glassy polymers. For example, the effect of deformation via uniaxial compression on the parameters of free volume of PMMA at room temperature was studied by the PALS method.[43] Typical results of this study are presented in Fig. 7. The parameter τ_3 of the PALS spectra related to the size of free volume holes increases with increasing strain even under the conditions of uniaxial compression.

As follows from Fig. 7, in the course of the plastic deformation, free volume holes in a glassy polymer

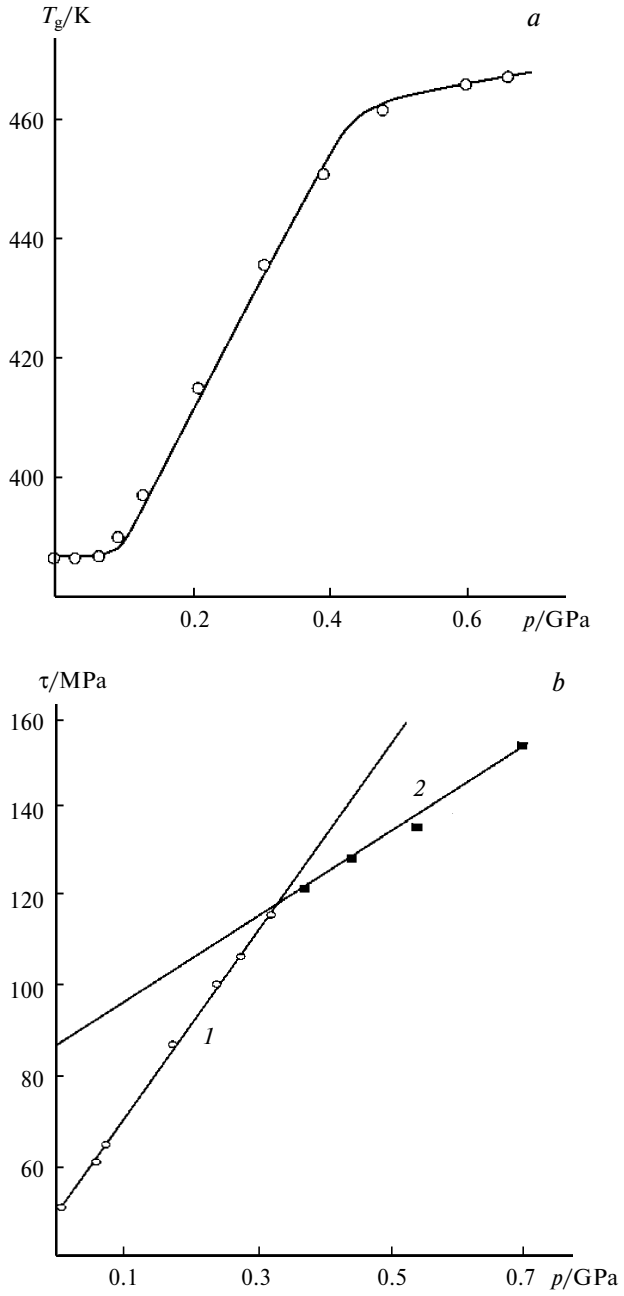

Fig. 6. Glass transition temperature[46] (*a*) and maximum shear stress (τ) (*b*) versus hydrostatic pressure (*p*) for PMMA at room temperature[18]. Straight line *1* depicts the change in the yield stress; straight line *2* shows the elongation at break.

increase their dimensions, probably, due to their merging (coalescence). Evidently, this merging cannot proceed for a long period of time; once a certain critical strain is attained, phase separation should commence. This process leads to the development of physical boundaries and real microvoids (cavities). Usually, cavitation in the deformed glassy polymer commences in the vicinity of the yield stress.

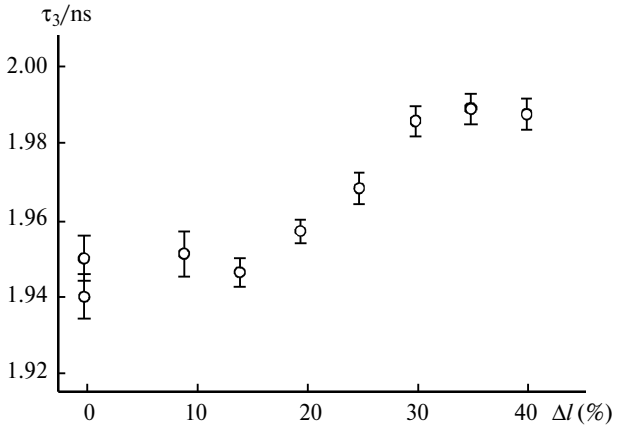

Fig. 7. Lifetime (τ_3) o-Ps versus strain (Δl) for uniaxial compression of PMMA at ~20°C.

Indeed, small-angle X-ray scattering data suggest that, even at strains below the yield point, certain new surfaces are formed in the deformed glassy polymer, which provide intensive X-ray scattering.[47] Transformation of free volume holes into real microvoids in the course of the orientational drawing of glassy polymers can be convincingly detected by visual observations. In particular, the formation of a neck in the polymer upon its tensile drawing is usually preceded by the development of a certain nucleation shear band (Fig. 8, *a*).[48] In the region corresponding to the transition of the deformed polymer into the neck, the development of several shear bands takes place (see Fig. 8, *b*); these shear bands have well-pronounced interfacial boundaries and the increased free volume content.[49]

Therefore, the increase in the free volume content upon plastic deformation of glassy polymers is accompanied not only by a marked increase in their specific volume but also by the development of well-pronounced interfaces. The development of the above boundaries is clearly detected in the transition region between undeformed bulk polymer and the formed neck (Fig. 9).[51] Even though the formed neck (see Fig. 9) has a fibrillar structure, it shows no marked small-angle X-ray scattering. Apparently, the fibrillar aggregates of macromolecules in the neck are so densely and perfectly packed that the neck contains no microvoids, which can be X-ray detected. The initial undeformed PET also does not show any marked small-angle X-ray scattering (see Fig. 9). Only in the transition region, intensive small-angle X-ray scattering is observed, and this fact attests that, within this region, polymer is disintegrated so that microvoids with dimensions of 5—10 nm and well-defined interfacial surfaces are formed.

Therefore, the following important assumption can be advanced: upon cold drawing, the transition of the polymer from unoriented to oriented state is accompanied by the loosening of the polymer and by the development of the structure with well-defined interfacial boundaries and real microvoids. In this connection, structural elements of the polymer that provide intensive small-angle X-ray scattering are assumed to be surfaces of fibrillar aggregates of oriented macromolecules, which are generated upon cold drawing of polymers.

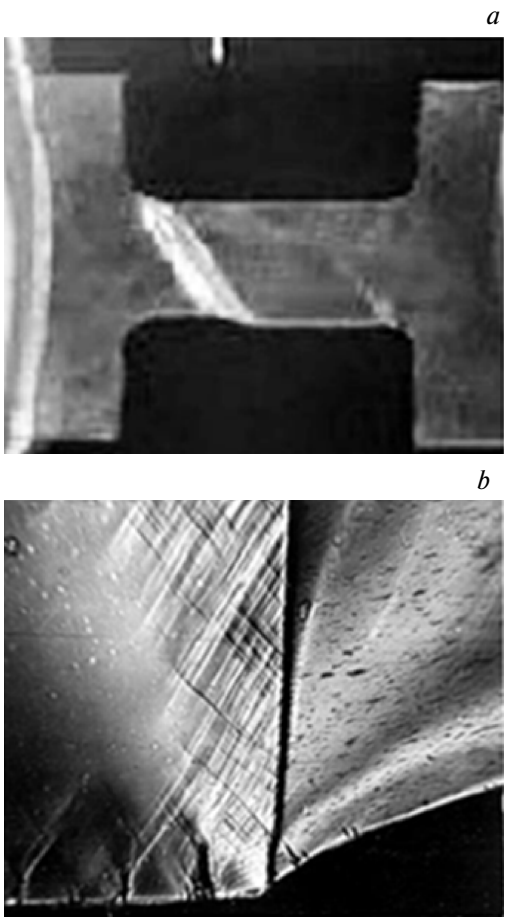

Fig. 8. (*a*) Visual appearance of the PC sample after its tensile drawing to the yield point[48] (×5); (*b*) micrograph of the region of the PET sample after necking[50] (×50).

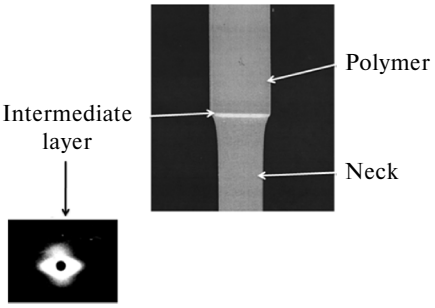

Fig. 9. The snapshot of the sample of amorphous glassy PET after its deformation via necking.[51] The inset (on the bottom left) shows the small-angle X-ray pattern of the intermediate layer between the neck and the undeformed part of the sample.

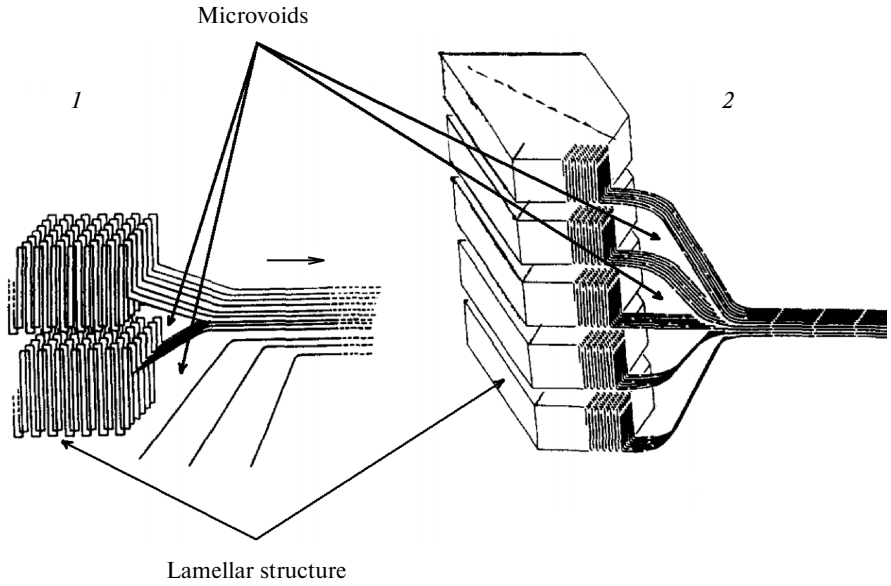

Fig. 10. Scheme illustrating the development of the fibrillar structure upon tensile drawing of the semicrystalline polymer according to the models by Kobayshi[53] (*1*) and by Reneker[54] (*2*).

Noteworthy is that the well-studied mechanism (as compared with glassy polymers) of tensile drawing of semicrystalline polymers (see, for example[52]) involves the development of the fibrillar structure and structural loosening upon its transition from the lamellar to the fibrillar structure. Figure 10 illustrates two models[53,54] for the description of the above structural transformation. According to these models, in the transition regions of the polymer located between oriented and unoriented (bulk) parts, microvoids are formed. Seemingly, there exists a certain geometrical demand for polymer loosening in the transition layer, and this process takes place before the formation of the fibrillar structure. This evidence highlights the key role of volume effects in plastic deformation of glassy polymers.

In the bottom line of this section, we would like to mention that a glassy polymer upon its deformation shows, at least, three morphological features: the development of a neck, crazes, and shear bands. This conclusion can be easily illustrated by direct microscopic observations. Figure 11 shows the optical micrograph of the sample after its loading within so-called region of elastic deformation (~0.7 of the yield stress). As follows from Fig. 7, when the sample is allowed to stay under stress, well-detected structural heterogeneities are developed in the sample. First, the micrograph shows the development of structural heterogeneities as linear bands, which are oriented perpendicular to the direction of the applied stress (so-called dry crazes); second, one can observe the network of structural heterogeneities as linear bands ori-

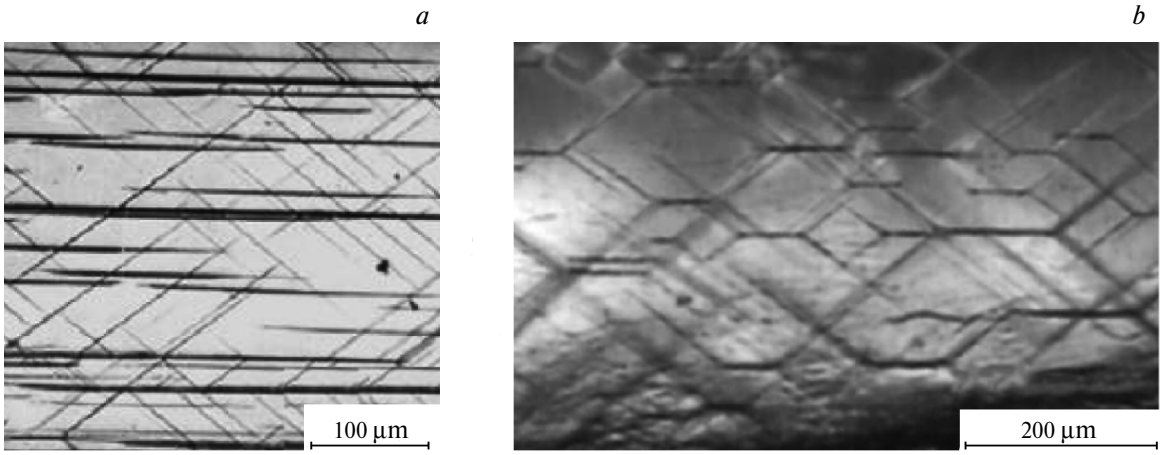

Fig. 11. Light micrograph of the PET sample after tensile drawing at room temperature at a constant stress of ~0.7 of the yield stress for 2 h[50] (*a*) and the electron micrograph of the transition region between the neck and the unoriented part of the PET sample[25] (*b*). In both cases, the axis of tensile drawing is vertical.

ented at an angle of ~45° with respect to the direction of the applied stress (shear bands) (see Fig. 11, *a*). Noteworthy is that, once the polymer is transformed into the neck, the above heterogeneities appear to be involved in the neck structure. The SEM micrograph illustrating the surface of the PET sample (Fig. 11, *b*) shows the well-defined shear bands and crazes produced in the unoriented part of the sample before its transition to the neck (see Fig. 11, *a*). Below, we will discuss in more detail the structure of crazes and shear bands; now, let us mention that all three above morphological forms are able to coexist in the structure of the glassy polymer upon its plastic deformation.

The effect of mechanical stress on the molecular mobility of glassy polymers

In the preceding section, the important role of volume phenomena upon plastic deformation of glassy polymers was discussed. However, this mode of plastic deformation is accompanied by the orientation of macromolecules, which, in turn, is undoubtedly related to the development of volume effects. Analysis of the mechanical properties of amorphous glassy polymers under stress impact allows one to reveal the key characteristics of the molecular mobility as a consequence of the mechanical impact on polymers. Let us consider some specific features of the stress-induced response of the glassy polymer upon its inelastic plastic deformation.

The studies on the dynamic mechanical properties of the polymer after its preliminary mechanical loading have revealed an evident structural heterogeneity of the deformed glassy polymer.[55—59] For example, inelastic deformation of the glassy polycarbonate (PC) was studied under uniaxial stretching coupled to simultaneous measurements of mechanical losses, which characterize the inner friction processes.

Figure 12 presents the stress—strain curve of the PC sample in comparison with the corresponding curve illustrating the parallel measurements of mechanical losses upon tensile drawing with a constant strain rate.[60,61] As follows from Fig. 12, at the initial stage (prior to mechanical loading), the mechanical losses are, as expected, low. Once the mechanical stress is applied, a "new" phase is developed in the polymer at tensile strains well below the yield strain (starting at a tensile strain of ~2%); this phase is characterized by a higher compliance and, hence, by higher mechanical losses. The content of this phase gradually increases with increasing tensile strain, and this behavior is associated with the concomitant growth of inner friction. This process is abruptly ceased once the yield point is attained. As the tensile strain is further increased (in the region where the neck is developed), no increase in the mechanical losses is observed; however, they do not decrease either. When the tensile drawing is

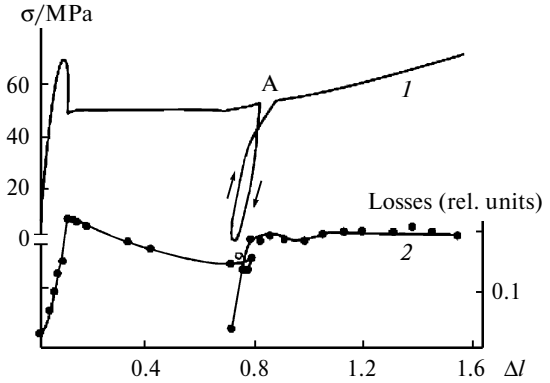

Fig. 12. The stress—strain curve (*1*) and the corresponding mechanical losses (*2*) in PC at ~20 °C. At the strain corresponding to point A in the stress—strain curve, the stress was decreased down to zero, and the sample was allowed to stay in this state for 1 h. After stress relaxation, tensile drawing was resumed.[60]

ceased in this interval of the stress—strain curve, stress relaxation is accompanied by a marked decrease in mechanical losses. This result unequivocally indicates relaxation (healing) of a "new" phase developed upon polymer deformation.

When the tensile drawing is resumed, the level of mechanical losses dramatically increases, and this fact attests a certain revival of the earlier relaxed regions with higher mechanical losses or the development of new regions. Noteworthy is that the content of these regions exactly corresponds to the level achieved upon the first loading run once the yield point is attained. This "phase" arises even at the so-called Hookean region of the stress—strain curve, and the content of this phase gradually increases up to the yield strain. Once the yield point is attained, the stress in the sample no longer increases, and the content of the "new" phase levels off. Therefore, the structure of the deformed glassy polymer is different from the structure of the initial polymer. Hence, one can assume that the initial structure of glassy polymers is not responsible for their abnormal physicochemical and physicomechanical behavior upon cyclic loading (see Fig. 12).

Let us consider this phenomenon in more detail. The samples of amorphous PC were subjected to uniaxial compression at ~2 °C by different strains; then, the samples were cooled by liquid nitrogen, and the temperature dependence of their dynamic mechanical characteristics was studied.[62] Figure 13 shows the temperature dependence of loss tangent at a loading frequency 1 Hz and at a scanning rate of 1 K/min for the samples after their plane compression by 0, 6, 10, 20, 30, and 40%.

For undeformed PC, the β- and α-relaxation processes are spaced by more than 200 °C; at this frequency, the α-peak is observed at 420 K. At the same time, the β-peak is located at 170 K and is seen to be broadened along the temperature axis since this peak is associated with a broad

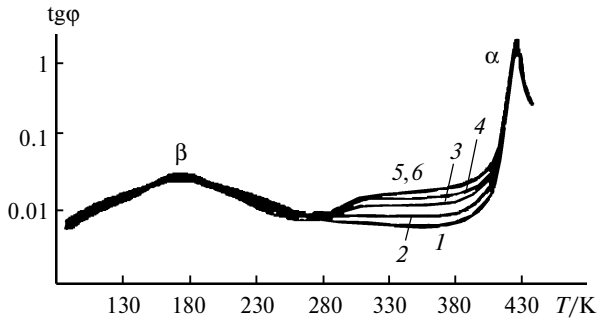

Fig. 13. The temperature dependence of loss tangent for PC samples after their deformation at room temperature under the conditions of uniaxial compression by 0 (*1*), 6 (*2*), 10 (*3*), 20 (*4*), 30 (*5*), and 40% (*6*).[62]

relaxation time distribution.[63,64] In the case of the deformed PC samples, in the interval between the α- and β-transitions, a broad relaxation transition spanning from 280 K up to T_g arises. This intermediate peak before the principal α-transition is fully eliminated when the polymer is annealed at temperatures above T_g, and its position is independent of the strain. As follows from Fig. 13, this transition is seen as a broad relaxation peak; later, this peak is transformed into the plateau which spans up to the principal α-transition. The height of this plateau increases with increasing strain but this growth is ceased at strains above 30%. The deformed glassy polymer is assumed to have certain "regions" where the molecular mobility is markedly enhanced as compared with that of initial bulk polymer. The development of the above "regions" with higher compliance provides unusual mechanical properties of the polymer. The above experimental results (see Figs 12 and 13) unequivocally indicate that plastic deformation of polymers leads to the development of the second "phase" with its specific properties. Noteworthy is that the appearance of the relaxation peak corresponding to the principal α-transition is provided by the deformation of the glassy polymer, and this behavior was also observed.[65,66]

Direct measurements of changes in the molecular mobility of the glassy polymer (weakly crosslinked poly(methyl methacrylate), PMMA) were performed by studying the intensity of the rotational molecular motion of low-molecular-mass probes in the polymer matrix at temperatures below T_g of the polymer (*optical photobleaching*).[67–71] This method allows *in situ* observations of the molecular rearrangements in polymers upon different modes of external impact (mechanical loading, relaxation, aging, *etc.*). According to the experimental evidence, plastic deformation markedly enhances the intensity of the molecular motion of the polymer (the intensity of the segmental mobility increases by a factor of 100 and higher). In the experiments, the samples with different prehistory (different degree of aging after temperature-induced rejuvenation) were used. At low strains (in the vicinity of the yield strain), aging and mechanical loading arise as two independent processes. Once the stress is released, the polymer sample rapidly relaxes down to its initial state. The above processes are most pronounced at strains corresponding to the yield point. Noteworthy is that the maximum intensity of the molecular motion is observed in the transition region between the neck and the unoriented state of the deformed polymer.

In the bottom line of this section, we will discuss the results of several works devoted to the study of the effect of the mechanical loading on the molecular mobility of glassy polymers by the method dielectric spectroscopy. For glassy polyvinyl chloride (PVC), this method allowed one to observe that the α- and β-relaxation transitions are markedly spaced along the temperature axis.[72] Upon mechanical loading, the intensity of these transitions increases, and their positions become closer. Mechanical loading of PMMA appears to have no effect on the position and intensity of the β-peak, whereas the mechanical α-losses are seen to be markedly enhanced.[73]

Therefore, mechanical loading leads to the development of a certain "phase" in the glassy polymer, and the peak at temperatures below the α-transition temperature (T_g) appears to be not only shifted to the region of low temperatures by tens of degrees but also is markedly broadened ("smeared") along the temperature axis.

Finally, let us mention that plastic deformation of glassy polymers is accompanied by a specific mode of their structuring, which is provided by the molecular mobility of the glassy polymer under the action of the external mechanical stress and by the free volume evolution in the strained polymer. Fibrillar structure of glassy polymers produced upon their cold drawing is likely to be the result of these structural rearrangements. However, the existing models describing the processes of plastic deformation of glassy polymers neglect the above structural behavior upon deformation of glassy polymers.

Free volume and physical (thermal) "aging" of glassy polymers

Glassy polymers also show another fundamental property, which is closely related to the free volume relaxation and, hence, to the large-scale molecular mobility within the temperature interval of the glassy state. This concerns the processes of so-called physical (thermal) aging of glassy polymers. Seemingly, within the temperature interval of the glassy state, large-scale molecular mobility is suppressed; however, the processes of physical aging are well known since long ago.

Let us consider the temperature dependence of the specific volume for the amorphous polymer (Fig. 14). When the temperature is decreased, the polymer in the

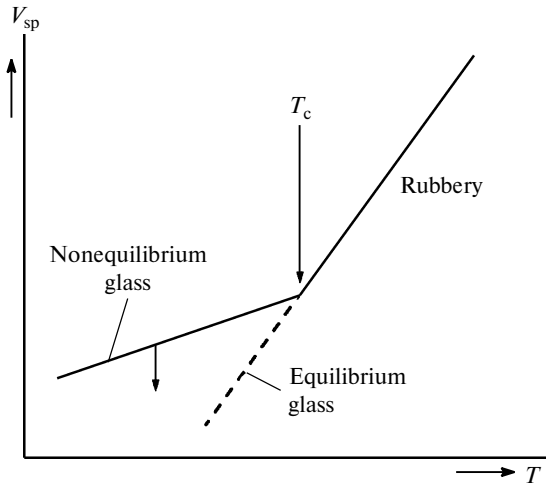

Fig. 14. Schematic representation of the temperature dependence of specific volume (V_{sp}) of amorphous polymer.

rubbery state decreases its specific volume since the volume of all solids decreases with decreasing temperature. Specificity of polymers is related to the fact that, as was mentioned above, their molecular mobility is critically different from that of low-molecular-mass solids. Since polymer molecules (macromolecules) are composed of long chains, their volume decreases not only due to the dense packing of individual molecules but also via shape changes (conformational changes) of these polymer chains. In other words, due to the flexibility of macromolecules, volume changes in the polymer are provided by the motion and mutual displacement of relatively long fragments of macromolecules, segments. Let us remind that this mode of segmental motion requires a certain free space.

At relatively high temperatures (in the rubbery state), polymer macromolecules or, to be more precise, their conformations exist in the equilibrium state since the free volume fraction and the related rate of structural rearrangements within this volume are high. As the temperature decreases, the rate of molecular rearrangements evidently becomes lower but remains high enough to keep the polymer in the state, which is close to the thermodynamic equilibrium. This scenery is preserved until the polymer approaches its T_g. Each polymer is characterized by its own T_g; however, once this temperature is attained, the polymer experiences the transition from the rubbery to glassy state (with decreasing temperature) and vice versa, from the glassy to rubbery state (with increasing temperature).

Once T_g is attained, the viscosity of the system dramatically increases, and the rate of molecular rearrangements is critically reduced; further temperature downturn does not allow the polymer to sustain equilibrium macromolecular conformations. The polymer has no time to attain the equilibrium state. Figure 14 shows that this behavior is accompanied by the marked change in the slope of the temperature dependence of the specific volume. The dotted line shows the trajectory depicting the decrease in the specific volume of the polymer with decreasing temperature provided the polymer is able to impart the equilibrium conformations to macromolecules. The data presented in Fig. 14 allow two following conclusions: first, the temperature dependence of the specific volume allows estimation of T_g of any amorphous polymer; second, on passing through T_g, the polymer appears to be in the thermodynamically non-equilibrium state. This statement is very important because any thermodynamic system in the non-equilibrium state tends to achieve or, at least, approach the equilibrium state. At the same time, as was mentioned above, at temperatures below T_g, segmental molecular motion responsible for polymer dynamics is prohibited.[17]

At temperatures well below T_g, the amorphous polymer is able to experience molecular rearrangements, which lead to marked changes in its characteristics. The direct proof of the occurrence of these rearrangements is provided, in particular, by the growth in polymer density, which spontaneously takes place with time upon aging of the freshly prepared and quenched (fast cooling below T_g) amorphous polymer. The example of this density growth in shown in Fig. 15:[74] upon isothermic aging, polymer volume markedly decreases as follows from the precise data of direct measurements of the linear dimensions of the polymer sample. The rate of this process (densification) depends on the aging temperature: the closer the annealing temperature to T_g, the higher the rate of this process. Let us emphasize that changes in the volume of the polymer sample upon its aging are the changes in the free volume. This result unequivocally sug-

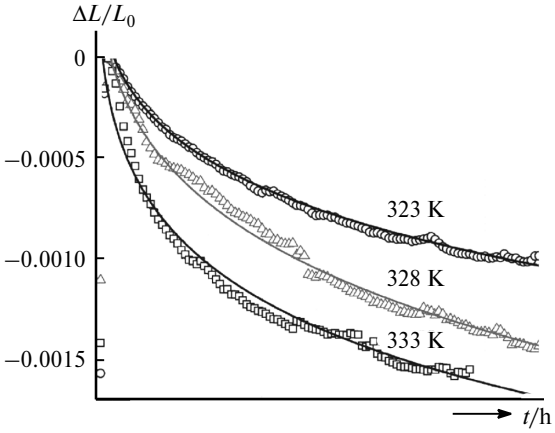

Fig. 15. Relative changes in linear dimensions ($\Delta L/L_0$) of the PET samples plotted against aging time (t) at constant temperature. The PET samples were quenched from the melt by cooling with ice water; then, the samples were heated to the temperatures shown at the curves with a heating rate of 10 K min^{-1} and subjected to isothermic annealing at temperatures below T_g of the polymer (T_g of PET is ~350 K).[74]

gests that aging processes in glassy polymers involve the temperature-activated molecular rearrangements; by themselves, these processes can take place at temperatures below T_g, or, in other words, in the temperature interval of the glassy state. Otherwise speaking, in the temperature region of the glassy state, molecular rearrangements are not prohibited but markedly retarded.

Noteworthy is that a certain "aging" process can be triggered in the polymer without any heating above glass transition temperature T_g, but, in the temperature interval of the glassy state, when the polymer is subjected to the mechanical impact, for example, to uniaxial compression or rolling of the polymer film. When the film of the "aged" glassy polymer is subjected to the above procedures, its characteristics are dramatically changed. Let us illustrate this phenomenon for the well-studied polymer such as PS (Fig. 16).[75] As follows from Fig. 16, preliminary mechanical treatment (in the case under study, rolling) leads to the phenomenon, which is similar to rejuvenation of the aged polymer upon heating above glass transition temperature followed by rapid cooling (quenching). In fact, the mechanically rejuvenated polymer has no yield tooth and subsequent stress relaxation. As is well known, under tensile drawing at room temperature, PC is the brittle material, and its fracture takes place at strains of about 1—2% (in the so-called Hookean region of the stress—strain curve). However, after the mechanical treatment, PS shows the ductile behavior, and its elongation at break at ~2°C achieves 30%.

For the strained polymer and for the polymer after its rejuvenation by heating above T_g and subsequent quenching (rapid cooling below T_g), annealing at temperatures above T_g leads to the complete recovery of all characteristics of the initial polymer and the effect of stress-induced rejuvenation is eliminated. Moreover, mechanically rejuvenated polymer spontaneously regains its initial mechanical properties without any annealing.

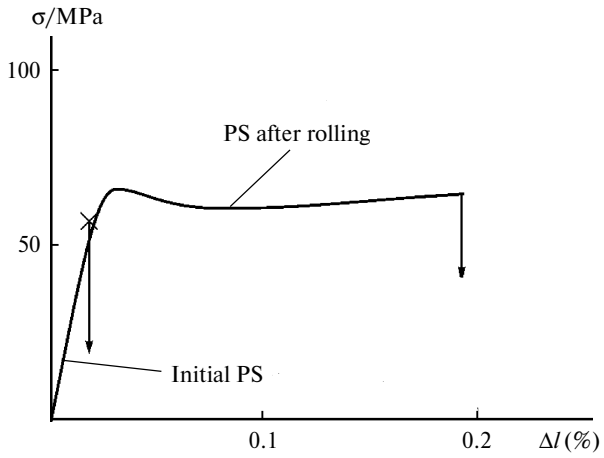

Fig. 16. The effect of rolling on the stress—strain curve of PS at room temperature. The arrows show the elongation at break.[75]

Therefore, there are two modes of rejuvenation of polymers, which are able to trigger the mechanism of aging: first, heating of the polymer above T_g followed by rapid cooling below this temperature (quenching) and, second, mechanical deformation in the temperature interval below T_g. Figure 17 shows the yield stress of the polymer plotted against the aging time after its rejuvenation by heating above T_g. In both cases, similar processes take place: yield stress spontaneously grows with time.

The following question arises: whether these two modes of aging involve similar molecular processes or structural changes with time are provided by different structural rearrangements? Since visual symptoms of aging phenomena induced by different factors are seen to be similar (see Fig. 17), this problem was the subject of numerous studies and discussions.[78] This question was clarified by the PALS studies of the free volume evolution for different modes of physical aging. In contrast to thermally rejuvenated samples, in this case, the decrease in free volume is totally controlled by the decrease in τ_3, whereas I_3 remains virtually unchanged.[79] Noteworthy is that invariable I_3 values upon aging convincingly validate the concept concerning the formation of a new phase in the

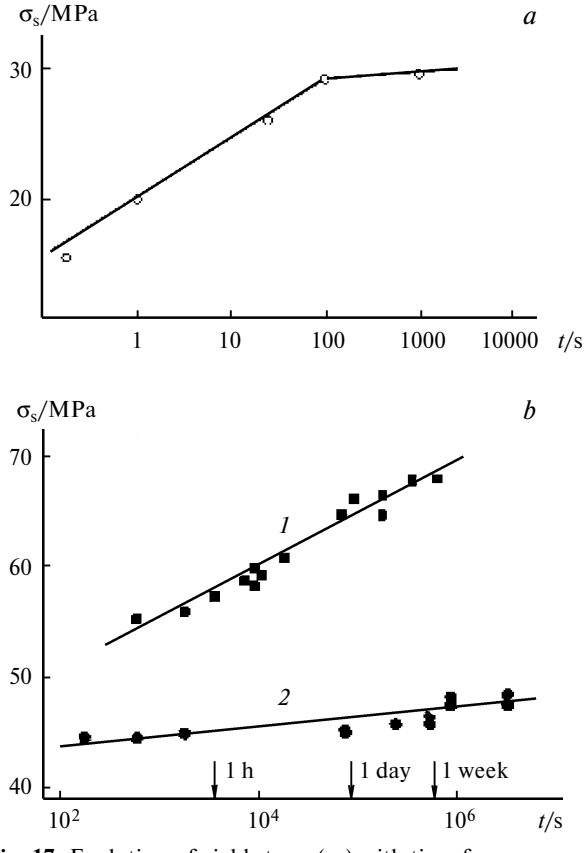

Fig. 17. Evolution of yield stress (σ_s) with time for epoxy resin after the thermal treatment at the temperature above T_g (*a*)[76] and for PS (*1*) and polycarbonate (PC) (*2*) after the preliminary rolling (*b*).[77]

plastically deformed glassy polymer, which has been advanced on the basis of the results of the mechanical tests.[60]

As follows from the above results, the properties of mechanically rejuvenated samples and the mechanism of their further relaxation are critically different from those of thermally rejuvenated samples. Therefore, analysis of the PALS data[79] justifies the idea[76] that aging of plastically deformed polymers is provided by the structural transition, which has been coined as an amorphous-amorphous transition. Undoubtedly, the above fibrillation is not a phase transition because, in this case, the polymer preserves its amorphous state. However, upon deformation of glassy polymers, the development of inner interfacial boundaries, which are typical of fibrillar aggregates of macromolecules, allows the assumption concerning the occurrence of the amorphous-amorphous structural transition, which is typical of fibrillation upon plastic deformation. At the same time, the popular idea concerning the mechanical rejuvenation advanced by Struik et al.[78] appears to be invalid. The effect of plastic deformation has been mistakenly interpreted as rejuvenation due to the phenomenon of subsequent aging, which is similar to the behavior after the temperature-induced rejuvenation. However, the key difference of the strain-induced aging is related to the reduced dimensions of free volume holes,[79] but their content remains unchanged in contrast to the scenario of aging after the temperature-induced rejuvenation. In other words, even though, in both cases, the macroscopic decrease in the volume of the polymer sample is the same, microscopic mechanisms behind this scenario are different.

Let us mention another structural feature, which highlights the difference between the polymer samples after rejuvenation via annealing at temperatures above T_g and further quenching and the polymer samples after the stress-induced rejuvenation. In the first case, rejuvenation is uniform (affine) throughout the whole polymer volume, whereas, in the second case, strain is heterogeneous (neck, crazes, or shear bands). Further aging of the above samples also proceeds via different pathways. After quenching, polymer changes its properties without any visible changes at the microscopic level. In the case of the mechanically rejuvenated polymer samples, aging proceeds via complete healing of the strain-induced microheterogeneities.

This property can be illustrated for the temperature-induced healing of shear bands in amorphous PET. The effect of annealing temperature on the state of shear bands in the polymer sample upon deformation under the conditions close to uniaxial compression was studied.[80] A spherical indentor tip was allowed to penetrate into the film of amorphous PET, and the induced pattern was studied by the light microscopy. Figure 18, *a* presents the micrograph of the deformed polymer sample after its annealing at a temperature of 40 °C, which is well below T_g. Under these conditions, deformation of the polymer sample is accompanied by the nucleation and development of the array of shear bands. As the annealing temperature is increased up to 70 °C (see Fig. 18, *b*), the shear bands appear to be more diffuse and less pronounced. Finally, when the annealing temperature approaches T_g (75 °C), shear bands are fully healed and cannot be detected by the light microscopic observations (see Fig. 18, *c*).

The low-temperature annealing (physical aging) of the polymer sample with shear bands is shown to provide a complete healing of interfacial surfaces, and this process primarily proceeds in the temperature interval below T_g. The low-temperature relaxation (below T_g of bulk polymer) is also observed for crazes.[50] It seems unexpected that, in PET, healing of shear bands proceeds in the temperature interval below T_g, where the large-scale molecular motion of the amorphous polymer is assumed to be frozen.[50] However, as will be shown below, for the glassy polymer in the highly dispersed state, T_g appears to be markedly depressed, and this depression is responsible for the observed structural rearrangements (see Fig. 18).

Therefore, the above literature evidence proves that, upon plastic deformation of glassy polymers, deep structural rearrangements take place. The principal features of these rearrangements are related to the fact that, in this case, strain is heterogeneously distributed within the polymer volume, and discrete zones with specific properties and well-defined interfacial boundaries are formed. The above structural heterogeneities are provided by the above

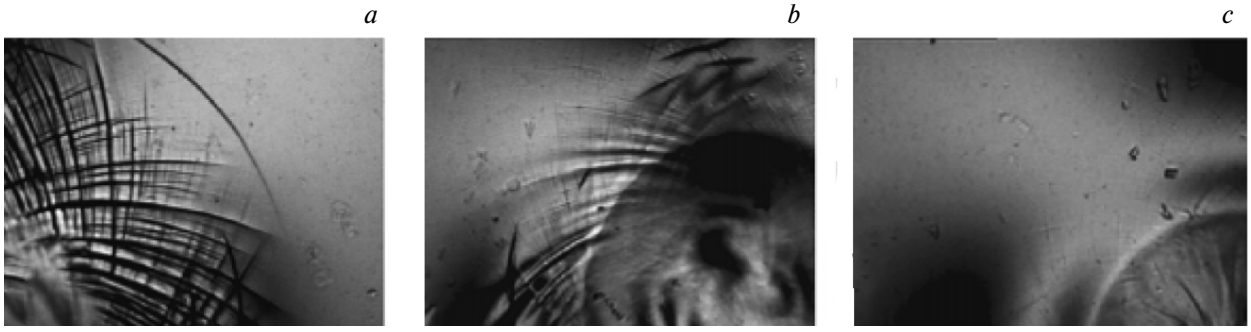

Fig. 18. Optical micrographs of the PET sample with shear bands after annealing at 40 (*a*), 70 (*b*), and 75°C (*c*).[81]

fibrillar structure, which is spontaneously produced upon deformation of glassy polymers.

The role of surface energy

Noteworthy is that the diameter of fibrillar aggregates of macromolecules, which are spontaneously produced in glassy polymers, ranges from several to tens of nanometers. This fact implies that polymer dispersed down to the nanoscale level is characterized by high interfacial surface (from tens to hundreds square meters per gram). This pattern exerts a marked effect on the character of structural rearrangements in the strained polymer. Indeed, the formation of a macroscopic neck proceeds via gradual transition of the polymer through the stage of dispersed state with the formation of physical interfacial boundaries between fibrillar structural elements with colloidal dimensions. At the same time, density of the oriented glassy polymers is usually higher than the density of bulk polymer; nevertheless, as was shown above, this material have well-pronounced interfibrillar interfaces.

This fact suggests that cold drawing of a glassy polymer proceeds in two stages (Fig. 19). Once the mechanical stress is applied to the polymer sample, the local free volume fraction increases at the stress concentration site, and this site serves as a nucleus for the localized plastic deformation; this nucleation site has the fibrillar structure (Fig. 19, sample *1*). Future life of this nucleation site depends on its level of interfacial surface energy. If this energy is high enough (for example, when the polymer sample is stretched in air), the assay of flexible polymer fibrils with the high level of interfacial surface energy merge (coagulate) into a monolithic neck (see Fig. 19, sample *2*). When the level of interfacial surface energy can be somehow reduced (for example, when the polymer sample is stretched in an adsorptionally active liquid environment (AALE)), coagulation of the fibrils appears to be markedly suppressed, and the polymer is able to preserve the high level of interfacial surface (see Fig. 19, sample *3*). This structural reorganization of the glassy polymer under the action of the applied stress has been coined as crazing. As a result of crazing, the polymer acquires new properties, which are not typical of the glassy state of amorphous polymers.[82]

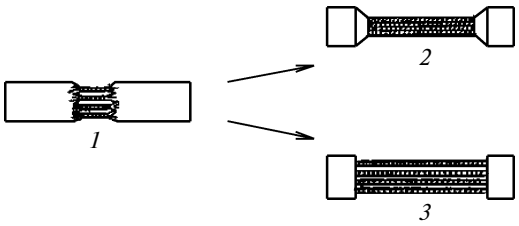

Fig. 19. Schematic representation of fibrillation in a glassy polymer (*1*) upon its deformation in air (*2*) and in the adsorptionally active liquid environment (*3*).[9]

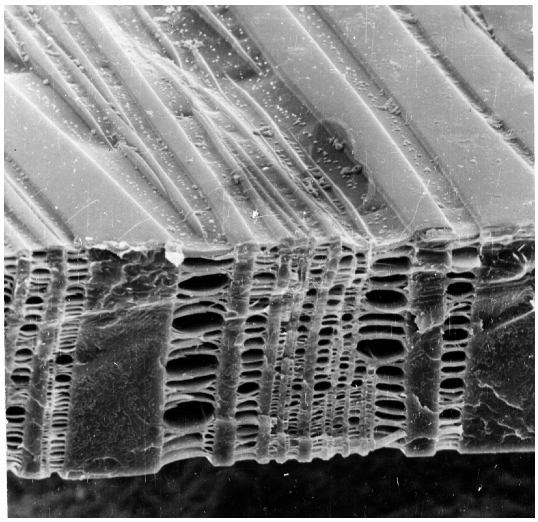

Fig. 20. Scanning electron micrograph of the fractured surface of the PET film after environmental crazing. The axis of tensile drawing is horizontal.[83]

Figure 20 presents the micrograph of the polymer sample after its tensile drawing in AALE, which markedly reduces its interfacial surface energy. In this case, instead of a monolithic neck (see Fig. 20), the polymer disintegrates into an assay of fibrillar aggregates of oriented macromolecules; as a result, the polymer acquires well-pronounced porosity and high level of interfacial surface.

Fibrillation of polymers in the course of crazing

As was mentioned above, the existing models of plastic deformation of glassy polymers ignore the phenomenon of polymer fibrillation. However, in the case of crazing, this phenomenon of fibrillation has been described in much detail. Let us consider some of the existing approaches. Deformation of the glassy amorphous polymer via the mechanism of crazing is the competition of two processes: on one hand, mechanical stress tends to expand the polymer sample (to generate the additional free volume) and, on the other hand, the action of surface tension forces, which tend to reduce the surface of the strained polymer. Numerous studies on the structure of the crazed polymers[82,84,85] show that, as a result of crazing, disordered amorphous polymer is spontaneously organized into an amazingly ordered and regular structure (Fig. 21).[86]

According to the general knowledge (see Fig. 21), orientational transformation of polymer upon deformation via the mechanism of crazing is accomplished within fibrillar aggregates bridging the fragments of initial amorphous unoriented polymer. When crazing is considered as a certain stability loss in the polymer system under the action of external forces, this approach allows a consistent explanation of the nucleation and development of

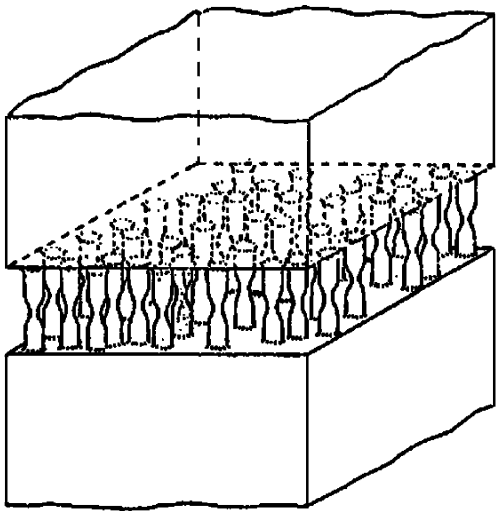

Fig. 21. Schematic representation illustrating the structure of a craze.[86] The axis of tensile drawing is vertical.

the unique structure of crazes. According to the modern concepts, this morphological transformation is based on the mechanism, which has been initially advanced for the explanation of the phenomena taking place upon mixing of two immiscible fluids with appreciably different densities.[87] This mechanism coined as the Rayleigh-Taylor meniscus instability can be explained as follows. When, under the action of external forces, two immiscible fluids move in a narrow channel, the interfacial boundary between them becomes unstable once a certain critical stress is attained. This instability manifests itself so that a fluid with a lower density penetrates a more viscous fluid and experiences disintegration into an assay of "thin fingers". Similar behavior is observed, for example, when a gap filled with a wetting liquid between two glass plates is opened (Fig. 22). In this case, under the action of surface forces, a fluid disintegrates into regular "fingers". This mechanism serves as the platform of crazing.[19] Under the deformation of the polymer, the external stress and counteracting hydrostatic pressure provided by the action of surface forces create the critical conditions when the polymer become involved in its spontaneous dispersion into the system of fibrillar aggregates.

Crazing of polymers is usually described and analyzed using the fundamental equation based on the theory of meniscus instability, which has been experimentally justified.[88] This equation relates the external stress σ and the diameter of the craze fibril d with specific surface energy of the polymer Γ

$$\sigma d = 8\Gamma(V_f)^{1/2},$$

where V_f is the volume fraction of fibrils in a craze.

The condition $\sigma d = const$ is the universal equation, which holds both for "dry" crazing[89] and for environmental crazing (solvent crazing).[90—92]

Noteworthy is that the necessary condition for the meniscus instability, which is responsible for the development of the highly dispersed fibrillar structure of crazes is the presence of a thin rubbery layer at the craze interface (Fig. 23). This layer is the locus where nucleation and development of the unique structure of a craze take place. When the theory explaining the formation of crazes has been worked out, the properties of polymers in thin layers were not studied well. By this reason, the assumption concerning the existence of a thin devitrified layer at the boundary between a growing craze and bulk polymer has been advanced (the layer thickness h, see Fig. 23). The formation of a thin (with a thickness of several nanometers) softened layer is related to the action of the expanding mechanical stress, which leads to the local

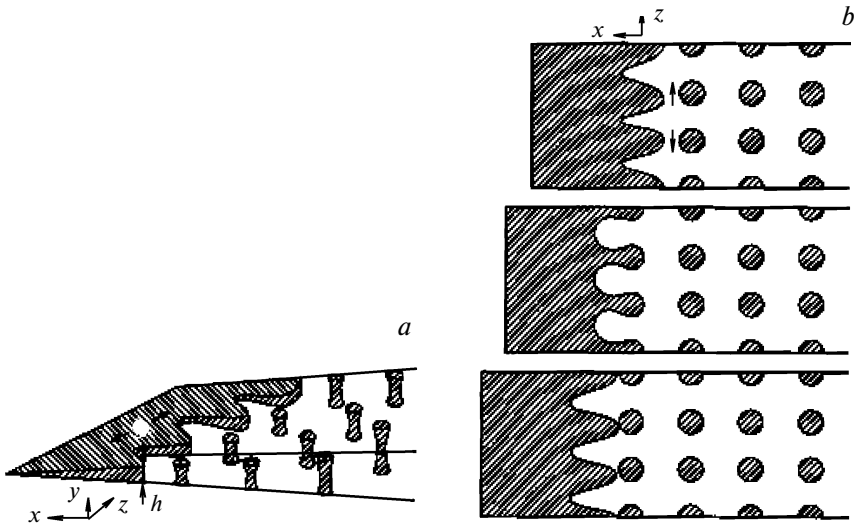

Fig. 22. Schematic representation of fibrillation upon crazing:[14] side view (*a)* and topside view (*b)*.

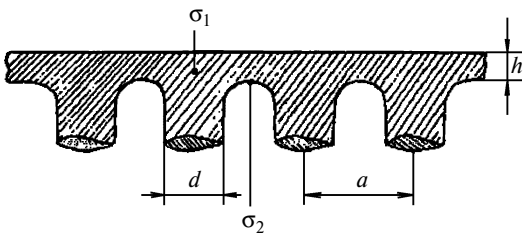

Fig. 23. Schematic representation illustrating the formation of fibrils upon crazing of a glassy polymer according to Kramer.[88]

increase in free volume. According to the literature data,[93] the above stress-induced softening can be so strong that, in the intermediate region, the polymer experiences devitrification and transition to the rubbery state. According to the concepts developed in the work,[88] the transition of the polymer into the softened rubbery state in a narrow layer adjacent to the craze wall provides the mechanical stability loss and, as a consequence, the development of a highly dispersed regular fibrillar structure. Below, we will discuss in more detail the structure and properties of amorphous polymers in thin films and surface layers. Now, we would only like to mention that the hypothesis concerning softening of a thin surface layer advanced in the works on the mechanism of crazing[88] has been splendidly proved in the works ten years later.

High plastic strain of a glassy polymer is always inhomogeneous within the volume of the polymer sample (the development of a neck, crazes, or shear bands). Evidently, the development of these regions of plastic deformation, in particular, crazes, requires the presence of certain microscopic heterogeneities in the initial polymer, which serve as nucleation sites for plastic strain localization. In this connection, let us mention that amorphous polymers are known to be structurally inhomogeneous solids containing structural heterogeneities with dimensions ranging from several to tens of angstroms.[94–96] In numerous studies, explanation of aging processes is based on the assumptions concerning inhomogeneous structure of polymer glasses and, in particular, the existence of certain ordered domains.[97–99] Structural inhomogeneity of amorphous polymers shows fluctuation non-equilibrium rather than phase character, and this fact creates marked difficulties for the experimental studies. The reasons behind the above difficulties are related to the prohibited use of direct structural methods based on the phase contrast of the objects under study (X-ray analysis, electron diffraction analysis). Numerous attempts to visualize structural heterogeneities (domains) in amorphous polymers by direct microscopic observations have been were reported. For example, structure of amorphous PS was studied by the electron diffraction method (the replica method) as a function of the duration of low-temperature annealing.[100] The grain character of polymer structure was observed, and this pattern becomes more pronounced with increasing temperature and duration of annealing (upon annealing, the dimensions of grains change from 300 to 700 Å). Increased dimensions of structural heterogeneities in the polymer have been also proved by the electron diffraction measurements. This study allows the conclusion that, in the course of physical aging, PS experiences structural rearrangements at the molecular level but their correlation with polymer properties was not established. Unfortunately, observations on structural inhomogeneity of polymers by K. Neki and P. H. Geil[100] did not allow an adequate representation of the structure of amorphous polymers.

The development of crazes was studied by the methods of molecular dynamics.[101] Microheterogeneities, which serve as stress-concentration sites, are presented as a set of inhomogeneities in the entanglement network (clusters) of the initial polymer as the regions with increased or, to the contrary, reduced density of entanglements. Clusters with the reduced density of the entanglement network serve as the sites for initiation and development of nanovoids at high stresses. The growth of voids proceeds via initiation of repeated events of cavitational instability over a growing cavity (a pore). This process is assisted by the disentanglement of the entanglement network and by the withdrawal of entanglements from the locus where the cavity is formed. In fact, mechanical energy is consumed for chain disentanglement, whereas the formation of stable fibrils requires low energy consumption. This approach offers an adequate explanation for crazing of polymers, which is illustrated in Fig. 24.

Fibrillation and shear flow of glassy polymers

In the preceding sections, the phenomenon of fibrillation of glassy polymers upon their cold drawing (necking) and crazing was analyzed. Noteworthy is that, in both

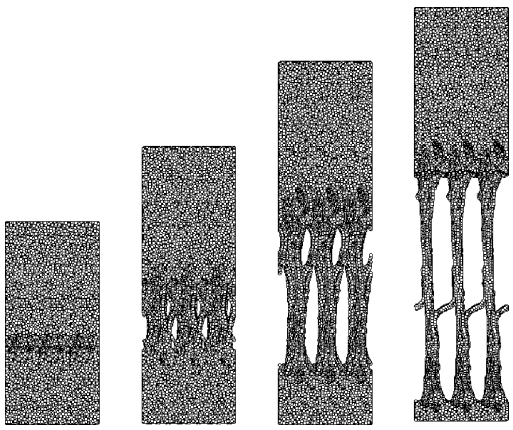

Fig. 24. Schematic representation illustrating the formation of crazes in the polymer with inhomogeneous entanglement network according to the molecular dynamics data.[101]

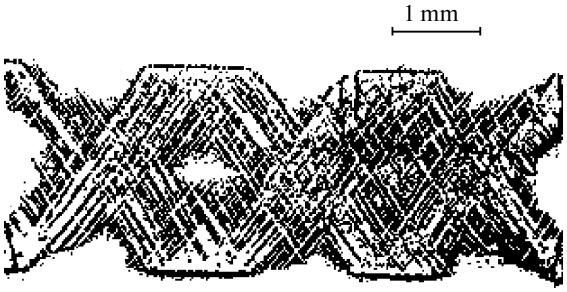

Fig. 25. Optical micrograph of a thin section of the PS sample after uniaxial compression. The axis of compression is vertical[102].

processes, fibrillation is primarily provided by the tensile component of the applied stress. At the same time, polymers can experience plastic deformation, for example, under the conditions of uniaxial compression in the temperature interval below T_g. The following question arises: whether fibrillation can take place when the polymer sample is subjected to this mode of deformation in the absence of the tensile stress component?

Let us consider in brief the scenario of structural rearrangements taking place in the polymer sample under uniaxial compression. In this case, strain appears to be inhomogeneously distributed within the volume of the glassy polymer.

As a rule, under uniaxial compression, a big-sized cylindrical sample acquires a barrel shape. The detection of any heterogeneities in the above samples becomes difficult. Nevertheless, the use of well-known techniques for the preparation of the samples for direct microscopic observations allowed the solution of the above problem. For example, the samples of several glassy polymers after their uniaxial compression were microtomed into thin sections.[102] The microtomed sections were studied by the polarization light microscopy. The microscopic observations reveal that the deformed glassy polymer (PS, PC, PET, PMMA) contains linear bands with a width of ~1 μm, which show strong birefringence and which are separated by the blocks of undeformed material. Figure 25 shows the micrograph of a thin section of the bulk PS samples after its uniaxial compression. The sample is seen to be saturated with shear bands. In other words, under the above conditions, deformation proceeds via the development of shear bands. Let us mention that a strong birefringence is observed not only for shear bands but also for crazes,[84] and this observation is indicative of the molecular orientation of the fibrillar material within these structural units.

Figure 26, *a* presents the image of the polymer sample with the shear band formed at the initial stage of tensile drawing.[103] Similar to low-molecular-mass solids, this band is seen to cross the sample at an angle of 45—50° with respect to the direction of tensile stress. However, this is the only common feature of shear bands in polymers and low-molecular-mass solids.

In polymers, shear bands are characterized by the complex structure.[104] They are stuffed with a highly dispersed fibrillar material, which is similar to the material within the volume of crazes.[82,84,86]

This crucial similarity is proved by direct microscopic observations. When the material containing shear bands is subjected to a slight stretching in the direction perpendicular to the plane of shear bands, they are opened (see Fig. 26, *b*) and the crazelike structure is revealed (cf. Figs. 20 and 26, *b*). In this case, the similarity with the craze structure appears to be so striking that the opened shear bands were referred to as *shear band crazes*. A certain morphological difference of a shear band craze and a classical craze is that, in the formed case, the fibrils are aligned at an angle with respect to shear band plane (see Fig. 26, *b*).

Complex fibrillar structure of shear bands in glassy polymers has a certain effect on the morphology of their

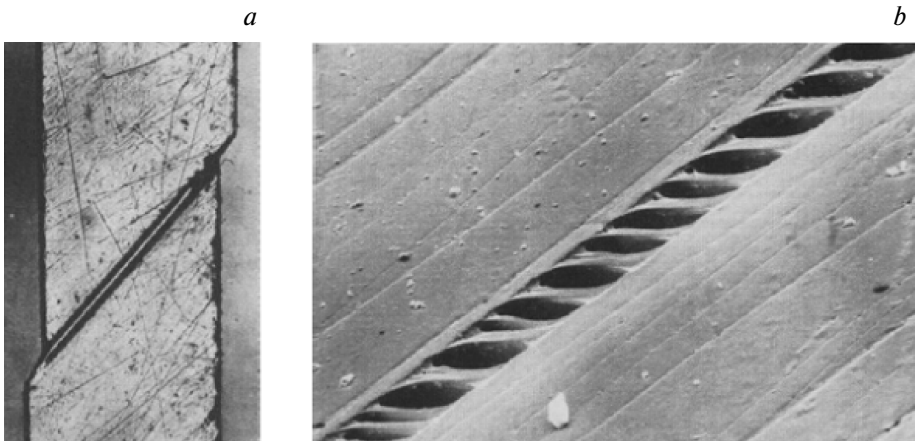

Fig. 26. Visual appearance of the PS sample with a shear band (*a*)[103] and the SEM image of the shear band (*b*) illustrating its inner structure[104].

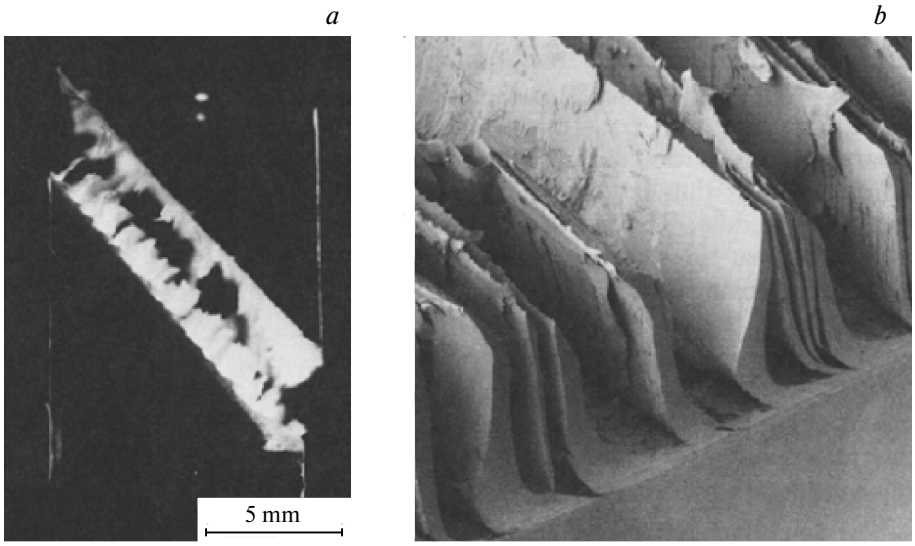

Fig. 27. Visual appearance of the PS sample (*a*) after its fracture along the shear band and SEM image of the fractured surface along the shear band (*b*).[104]

fractured surfaces. Figure 27, *a* shows the micrograph of the PS sample with the initiated shear band. Further deformation leads to the fracture of the sample along this shear band. In this case, within the volume of the shear band, numerous zones of plastically deformed polymer are formed. At high magnifications (see Fig. 27, *b*), this material is seen to contain parallel lamellas formed by the coagulated fibrils. By its morphology, this structure is similar to the craze matter, which has been revealed for the fractured surfaces of the crazed polymers.[83]

In the work by Li,[104] a shear band and a craze were produced in one and the same PS sample. Figure 28 presents the SEM image of this sample. In contrast to a classical craze, fibrils in a shear band craze are aligned at an angle with respect to the shear band plane. All other morphological features of both structures are fully the same.

Another important feature of structural microheterogeneities (shear bands and crazes) induced by deformation of glassy polymers is related to the presence of real microvoids. At the present time, the existence of microporous strcuture in crazes is beyond any doubts.[50] Deformation of polymers in the presence of AALE proceeds, at least, at the early stages, via the growth of the overall porosity. At the same time, shear yielding is accompanied by a marked contraction of the stretched polymer and, despite the presence of shear bands with real interfaces, the question concerning the development of the porosity in the polymer sample is still unclear.

As was shown by Harmon et al.,[105] transport of methanol into the PMMA samples after their uniaxial compression by 23—24% appears to be substantially different from the transport into the initial undeformed polymer. As compared with undeformed PMMA, the diffusion rate appears to be two times higher at 40 °C and five times higher at 25 °C. This evidence suggests that, in glassy polymers, shear bands contain certain regions stuffed with loosened material which allows enhanced transport of low-molecular-mass substances.

There is a simple pathway to demonstrate how, under the same conditions, deformation of the polymer proceeds via crazing or via the development of shear bands.[106] When the bulk PET samples are stretched in the AALE, crazes are initiated at their surface and grow into the depth of the sample. Evidently, in the course of the craze growth, hydrostatic resistance to the liquid flow towards the craze tip is enhanced. Finally, the liquid cannot effectively penetrate to the sites of the orientational transformation (craze tips) in sufficient amounts. Since the growth of crazes necessitates the presence of the AALE at the active deformation sites, the polymer prefers an

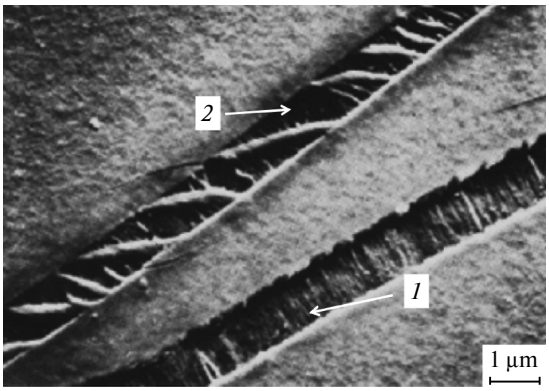

Fig. 28. SEM image of the PS sample with a craze (*1*) and a shear band (*2*).[104]

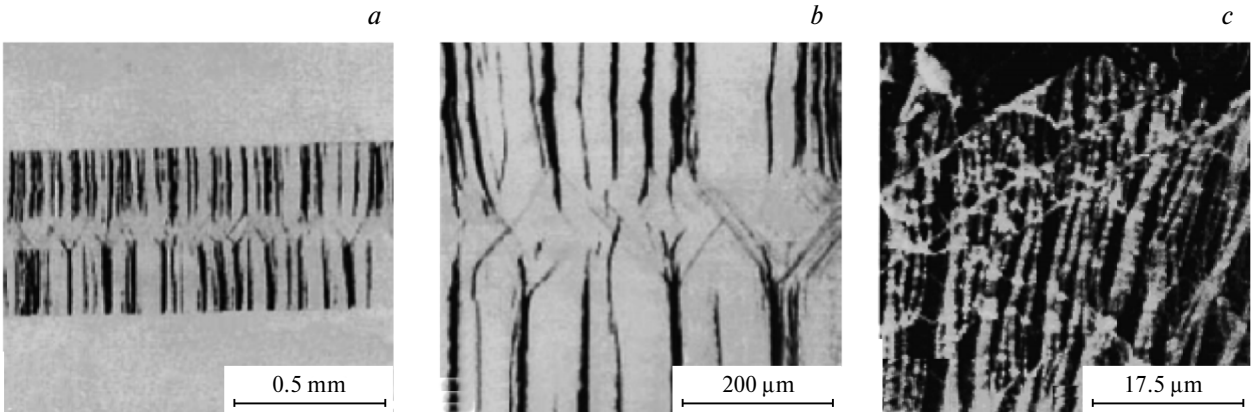

Fig. 29. Optical micrograph of the thin section of the PET sample containing crazes and shear bands (*a*, *b*). The SEM image of the low-temperature fractured surface of the same PET sample after its use as a membrane in the dialysis cell containing aqueous solutions of NaCl and $AgNO_3$ (*c*).[106] Comments are given in the text.

alternative pathway via the mechanism of the growth of shear bands.

This scenario is illustrated in Fig. 29, which shows the light micrograph of a thin section of the PET sample with a thickness of 0.7 mm after its tensile drawing at room temperature in the AALE (*n*-hexanol) by 50% with a strain rate of ~100% min^{-1}. Under the above conditions, the crazes are unable to pass the whole cross section of the polymer sample and to proceed to the stage of craze widening (craze thickening) (see Fig. 29, *a*); however, in its central part, the polymer sample continues its deformation via the growth of shear bands, which requires no presence of the AALE. At higher magnifications (see Fig. 29, *b*), the micrographs reveal some important features of this deformation mode. Similar to crazes, shear bands are well visualized in the light microscopic observations, and this fact indicates the presence of well-defined interfacial boundaries.

Figure 29 shows the image of the cross section of film which was placed as a membrane in the dialysis cell between the chambers filled with the aqueous solution of NaCl, on one side, and $AgNO_3$, on the other side. When crazes cross the whole cross section of the polymer film, solutions of NaCl and $AgNO_3$ diffuse towards each other through the system of interconnected pores, come into contact, and yield AgCl crystals, which can be easily detected by the electron scanning microscopy.[107] As follows from Fig. 29 (*a* and *b*), the bulk PET film after its tensile drawing in the AALE is characterized by unusual layered structure. Crazes containing real microvoids do not penetrate the whole cross section of the polymer sample but leave the intact layer in the core of the film, which contains no crazes but is seen to be crossed by shear bands.

Figure 29, *c* shows the SEM image of the fractured surface of the same PET sample after the treatment via the countercurrent diffusion with NaCl and $AgNO_3$ solutions. As a result of this procedure, the light-colored AgCl crystals are produced in the volume of crazes, and this fact indicates the complete penetration of NaCl and $AgNO_3$ solutions through the PET film. Moreover, the images in Fig. 29 show that the AgCl crystals are precipitated not only within the microvoids of crazes but also within the shear bands (linear channels crossing the polymer at an angle of ~45°), thus contrasting them. This result unequivocally suggests that even though the shear bands do not contain real microvoids, they have a lowered density so that a low-molecular-mass liquid can diffuse along them as through the channels.

In the conclusion of this section, let us highlight the striking similarity between crazes and shear bands. This similarity can be formulated as follows: shear bands and crazes are through channels filled with the highly dispersed material. As was mentioned above, there is no critical difference between the structure of crazes and shear bands. In both cases, structural units with fibrillar

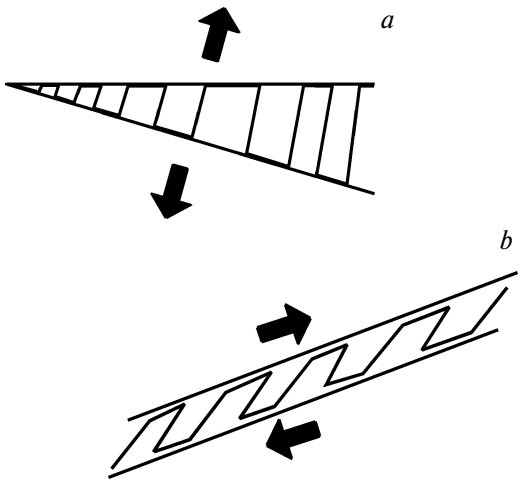

Fig. 30. Schematic representation illustrating the structure of a craze (*a*) and a shear band (*b*).[108]

morphology and, hence, with a high level of interfacial surface are formed. This conclusion was illustrated by the following example[108] (Fig. 30). In this connection, it makes no difference whether deformation proceeds via the development of shear bands or crazes. In both cases, the polymer acquires the excessive interfacial surface, which is typical of the fibrillar structure of shear bands or crazes.

On certain properties of fibrillar polymers

Therefore, plastic deformation of glassy polymers proceeds via the development of, at least, three morphological forms: a neck, crazes or shear bands. All modes of deformation lead to the development of the fibrillar morphology in the polymer sample.

Naturally, this complicated structural organization of the deformed glassy polymers manifests itself in their macroscopic characteristics. Indeed, the deformed glassy polymers show numerous abnormalities in their structural mechanical behavior.[64] After their deformation in the glassy state, amorphous polymers experience well-pronounced stress relaxation in the so-called elastic region of the stress—strain curve,[109] stress rise upon isometric annealing in the temperature interval below T_g.[110,111] These polymers recover their initial dimensions at temperatures below glass transition temperature or, in other words, under the conditions when the large-scale molecular motion should be suppressed.[46,112—115] The strained amorphous polymers show abnormal dynamic mechanical properties. Numerous works[55,56,58—60,62,63,65,66,116,117] convincingly prove that the deformed glassy polymer is able to experience large-scale molecular motion at temperatures by tens of degrees lower than their T_g. Numerous thermodynamic studies by the deformation calorimetry[113—115] show that plastic deformation of glassy polymers is critically different from the corresponding process in the low-molecular-mass solids. Most of deformation work (primarily prior to yield stress and in the region of yielding) is accumulated by the polymer rather than transformed to heat.

To summarize, we can draw the conclusion that deformation of glassy polymers accompanied by their fibrillation triggers the low-temperature (below T_g) large-scale molecular motion. The question concerning the mechanism of the above phenomena arises. This question can be clarified by the finding discovered in the middle of the 1990s: the dependence of glass transition temperature of amorphous polymers on the dimensions of the polymer phase. At the present time, the fact that such fundamental property as T_g of the amorphous polymer is not invariable, ys beyond any doubts. As the dimensions of the polymer phase are reduced down to the nanoscale level, T_g of the polymer appears to be markedly depressed (Fig. 31).[118,119]

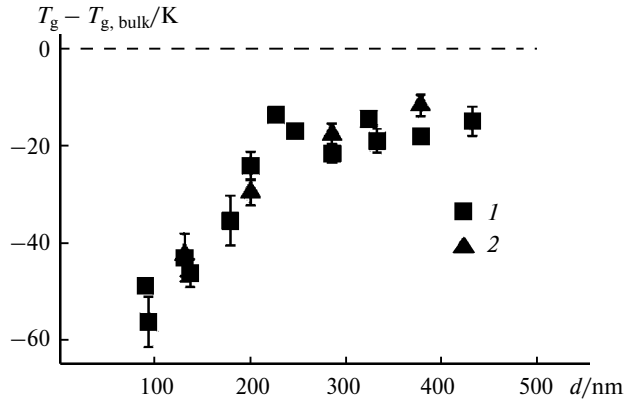

Fig. 31. Depression in glass transition temperature of polystyrene nanoparticles plotted against their dimensions: DSC measurements (*1*) and dilatometric measurements (*2*). The dotted line corresponds to T_g of the bulk PS.[118]

Glass transition temperature T_g of the polymer decreases by many tens of degrees when the polymer phase falls into nanoscale dimensions. Noteworthy is that this depression in T_g is observed not only for nanoparticles but also for thin polymer films[120—122] and fibers.[123] As was shown above, the diameter of fibrillar aggregates of macromolecules ranges from several to tens of nanometers and, hence, they are characterized by a sufficiently low T_g as compared with that of the surrounding bulk polymer. In essence, the development of fibrillar aggregates of macromolecules (fibrils) in the bulk polymer means the introduction of a certain component with fibrillar morphology and depressed T_g. The account for this scenario allows universal explanation of the above abnormalities in the structural mechanical behavior of glassy polymers.[64]

Conclusion

Therefore, analysis of the literature data allows the conclusion that plastic deformation of glassy polymers is accompanied by a certain structural transformation, which leads to the development of the fibrillar structure in the polymer. This structure features the aggregates of oriented macromolecules with the diameter ranging from several to tens of nanometers. The development of this morphology is related to the competition between two oppositely directed forces: on one hand, the mechanical stress that tends to increase the volume of the polymer sample and, on the other hand, the surface tension forces that tend to reduce the volume of the polymer sample. As a result of this conflict, the polymer disintegrates down into the assay of oriented aggregates (fibrils). For the above phenomenon of polymer self-dispersion, of special emphasis is the important role of interfacial surface energy. When the interfacial tension is reduced, for example, using the AALE, the system of nanoscale aggre-

gates (fibrils) appears to be stabilized, and the process is directed according to the scenario of crazing, which involves the development of high porosity and high interfacial surface. Due to the high level of interfacial surface energy, for example, when the polymer is stretched in air, the highly dispersed system becomes unstable; as a result, nanoscale fibrils tend to reduce their interfacial energy and merge (coagulate) into a monolithic neck.

This work was financially supported by the Russian Science Foundation (Project No. 17-13-01017).

References

1. A. L. Volynskii, N. B. Zmienko, N. F. Bakeev, *Polym. Sci. USSR* (*Engl. Transl.*), 1971, **13**, 47.
2. C. D. Vacogne, S. M. Brosnan, A. Masic, H. Schlaad, *Polymer Chem.*, 2015, **6**, 5040.
3. A. Rahy, M. Sakrout, S. Manohar, S. J. Cho, J. Ferraris, D. J. Yang, *Chem. Mater.*, 2008, **20**, 4808.
4. D. Roy, J. T. Guthrie, S. Perrier, *Soft Matter*, 2008, **4**, 145.
5. S. Virtanen, J. Vartianen, H. Setala, T. Tammelin, S. Vuoti, *RSC Adv.*, 2014, **4**, 11343.
6. R. G. Zhbankov, P. V. Kozlov, *Physics of Cellulose and Its Derivatives*, Nauka i Tekhnika, Minsk, 1983, 296 p.
7. M. Janko, A. Zink, A. M. Gigler, W. M. Heckl, R. W. Stark, *Proc. R. Soc., Ser. B: Biol. Sci.*, 2010, **277**, 2301.
8. W. Yang, V. R. Sherman, B. Gludovatz, E. Schaible, P. Stewart, R. O. Ritchie, M. A. Meyers, *Nat. Commun.*, 2015, **6**, 6649.
9. A. L. Volynskii, N. F. Bakeev, *Vysokodispersnoe orientirovannoe sostoyanie polymerov* [*Highly Dispersed Oriented State of Polymers*], Khimiya, Moscow, 1984, 190 p. (in Russian).
10. P. V. Kolluru, I. Chasiotis, *Polymer*, 2015, **56**, 507.
11. D. Sikorski, *Fibre Structure*, Ed. R. H. Peters, J. W. S. Hearle, Butterworths, London, 1963, 421 p.
12. S. N. Zhurkov, V. A. Marikhin, L. P. Romankova, A. I. Slutsker, *Polym. Sci. USSR* (*Engl. Transl.*), 1962, **4**.
13. V. S. Kuksenko, O. D. Orlova, A. I. Slutsker, *Polym. Sci. USSR* (*Engl. Transl.*), 1973, **15**, 2849].
14. A. Peterlin, *Int. J. Fracture*, 1975, **11**, 761.
15. P. H. Geil, *Polymer Monocrystal,* Wiley, New York, 1958.
16. G. Schuur, A. K. Van Der Vegt, *Orientation of Films and Fibrillation,* in *Structure and Properties of Oriented Polymers*, Ed. I. M. Ward, Springer Netherlands, Dordrecht, 1975, p. 413.
17. V. N. Kuleznev, V. A. Shershnev, *Khimiya i fizika polimerov* [*Chemistry and Physics of Polymers*], KolosS, 2007, 368 pp. (in Russian).
18. I. M. Ward, J. Sweeney, *An Introduction to the Mechanical Properties of Solid Polymers,* John Wiley&Sons, Chichester, 2004, 394 p.
19. A. S. Argon, *The Physics of Deformation and Fracture of Polymers*, Cambridge University Press, 2013, 532 p.
20. J. Perez, *Physics and Mechanics of Amorphous Polymers*, Ed. A. A. Balkema, Publisher, Rotterdam, 1998, 324 p.
21. G. M. Bartenev, Yu. V. Zelenev, *Entsiklopediya polimerov* [*Encyclopedia of Polymers*], Isd. Sov. entsiklopediya, 1972 **1**, 722 pp. (in Russian).
22. G. M. Bartenev, S. Ya. Frenkel´, *Fizika polimerov* [*Physics of Polymers*], Khimiya, Leningrad, 1990, 432 pp. (in Russian).
23. J. T. A. Kierkels, *Tailoring the Mechanical Properties of Amorphous Polymers*, Technische Universiteit Eindhoven, Eindhoven, 2006, 138 p.
24. L. R. G. Treloar, *The Physics of Rubber Elasticity,* Clarendon Press, Oxford, New York, 2005, 310 p.
25. C. G´Sell, J. M. Hiver, A. Dahoun, *Int. J. Solids Struct.*, 2002, **39**, 3857.
26. W. Whitney, R. D. Andrews, *J. Polym. Sci., Part B: Polym. Symp.*, 1967, **16**, 2981.
27. D. M. Schrader, Y. C. Jean, *Positron and Positronium Chemistry,* in *Studies in Physical and Theoretical Chemistry*, Elsevier, 1988, **57**, 395 p.
28. M. Eldrup, D. Lightbody, J. N. Sherwood, *Chem. Phys.*, 1981, **63**, 51.
29. V. P. Shantarovich, *J. Radioanalyt. Nucl. Chem.*, 1996, **210**, 357.
30. C. Wästlund, F. H. J. Maurer, *Polymer*, 1998, **39**, 2897.
31. J. Zrubcová, J. Krištiak, W. B. Pedersen, N. J. Pedersen, M. M. Eldrup, *Mater. Sci. Forum*, 2001, **363—365**, 359.
32. G. Alba, L. D. A. Siebbeles, H. Schut, A. van Veen, *Radiat. Phys. Chem.*, 2003, **68**, 515.
33. D. Cangialosi, H. Schut, M. Wübbenhorst, J. van Turnhout, A. van Veen, *Radiat. Phys. Chem.*, 2003, **68**, 507.
34. C. L. Wang, K. Hirata, J. Kawahara, Y. Kobayashi, *Phys. Rev. B*, 1998, **58**, 14864.
35. F. H. J. Maurer, M. Schmidt, *Radiat. Phys. Chem.*, 2000, **58**, 509.
36. M. Welander, F. H. J. Maurer, *Mater. Sci. Forum*, 1992, **105—110**, 1811.
37. L. Xie, D. W. Gidley, H. A. Hristov, A. F. Yee, *J. Polym. Sci., Part B: Polym. Phys.*, 1995, **33**, 77.
38. S. J. Tao, *J. Chem. Phys.*, 1972, **56**, 5499.
39. Y. Kobayashi, W. Zheng, E. F. Meyer, J. D. McGervey, A. M. Jamieson, R. Simha, *Macromolecules*, 1989, **22**, 2302.
40. A. J. Hill, M. Katz, P. L. Jones, *Polym. Eng. Sci.*, 1990, **30**, 762.
41. Q. Deng, F. Zandiehnadem, Y. C. Jean, *Macromolecules*, 1992, **25**, 1090.
42. J. E. Kluin, Z. Yu, S. Vleeshouwers, J. D. McGervey, A. M. Jamieson, R. Simha, K. Sommer, *Macromolecules*, 1993, **26**, 1853.
43. O. A. Hasan, M. C. Boyce, X. S. Li, S. Berko, *J. Polym. Sci., Part B: Polym. Phys.*, 1993, **31**, 185.
44. A. E. Hamielec, M. Eldrup, O. Mogensen, *J. Macromol. Sci., Part C*, 1973, **9**, 305.
45. A. D. Kasbekar, P. L. Jones, A. Crowson, *J. Polym. Sci., Part A: Polym. Chem.*, 1989, **27**, 1373.
46. M. S. Arzhakov, S. A. Arzhakov, G. E. Zaikov, *Structural and Mechanical Behavior of Glassy Polymers*, Nova Science Pubishers, New York, 1997, 275 p.
47. Yu. S. Nadezhdin, A. V. Sidorovich, B. A. Asherov, *Polym. Sci. USSR* (*Engl. Transl.*), 1976, **18**, 2995.
48. J. Sweeney, P. Caton-Rose, R. Spares, P. D. Coates, *J. Appl. Pol. Sci.*, 2007, **106**, 1095.
49. A. A. Berlin, M. A. Mazo, I. A. Strel´nikov, N. K. Balabaev, *Polym. Sci., Ser. D*, 2015, **8**, 85.
50. A. L. Volynskii, N. F. Bakeev, *Rol´ poverkhnostnykh yavlenii v strukturno-mekhanicheskom povedenii tverdykh poli-*

merov [*The Role of Surface Phenomena in Structural Mechanical Behavior of Solid Polymers*], Fizmatlit, Moscow, 2014, 536 pp. (in Russian).
51. A. L. Volynskii, Thesis. Doctor of chemical sciences, MGU, Moscow, 1979 (in Russian).
52. A. Peterlin, *Colloid. Polym. Sci.*, 1987, **265**, 357.
53. K. Kobayashi, in *Polymer Single Crystals*, Ed. P. Geil, Interscience, New York, 1963, 473 p.
54. D. H. Reneker, J. Mazur, *Polymer*, 1983, **24**, 1387.
55. M. L. Wallace, B. Joos, *Phys. Rev. Lett.*, 2006, **96**, 025501.
56. C. Gauthier, J. M. Pelletier, L. David, G. Vigier, J. Perez, *J. Non-Cryst. Solids*, 2000, **274**, 181.
57. I. V. Fadeeva, E. S. Trofimchuk, M. Giretova, D. K. Mal´tsev, N. I. Nikonorova, A. S. Fomin, J. V. Rau, L. Medvecky, S. M. Barinov, *Biomed. Phys. Eng. Express*, 2015, **1**, 045011.
58. E. Munch, J.-M. Pelletier, B. Sixou, G. Vigier, *Phys. Rev. Lett.*, 2006, **97**, 207801.
59. M. Warren, J. Rottler, *J. Chem. Phys.*, 2010, **133**, 164513.
60. J. Parisot, O. Rafi, W. J. Choi, *Polym. Eng. Sci.*, 1984, **24**, 886.
61. H.-N. Lee, K. Paeng, S. F. Swallen, M. D. Ediger, *J. Chem. Phys.*, 2008, **128**, 134902.
62. E. Munch, J.-M. Pelletier, G. Vigier, *J. Polym. Sci.*, *Part B: Polym. Phys.*, 2008, **46**, 497.
63. S. Havriliak, T. J. Shortridge, *Polymer*, 1990, **31**, 1782.
64. A. L. Volynskii, L. M. Yarysheva, N. F. Bakeev, *Rev. J. Chem.* (*Engl. Transl.*), 2012, **2**, 171.
65. C. Bauwens-Crowet, *Mater. Sci.*, 1999, **34**, 1701.
66. A. R. Berens, I. M. Hodge, *Macromolecules*, 1982, **15**, 756.
67. B. Bending, M. D. Ediger, *J. Polym. Sci.*, *Part B: Polym. Phys.*, 2016, **54**, 1957.
68. K. Hebert, B. Bending, J. Ricci, M. D. Ediger, *Macromolecules*, 2015, **48**, 6736.
69. B. Bending, K. Christison, J. Ricci, M. D. Ediger, *Macromolecules*, 2014, **47**, 800.
70. H.-N. Lee, M. D. Ediger, *J. Chem. Phys.*, 2010, **133**, 014901.
71. H.-N. Lee, M. D. Ediger, *Macromolecules*, 2010, **43**, 5863.
72. J. Kalfus, A. Detwiler, A. J. Lesser, *Macromolecules*, 2012, **45**, 4839.
73. A. Aref-Azar, J. N. Hay, *Polymer*, 1982, **23**, 1129.
74. K. Sato, W. Sprengel, *J. Chem. Phys.*, 2012, **137**, 104906.
75. L. E. Govaert, H. G. H. van Melick, H. E. H. Meijer, *Polymer*, 2001, **42**, 1271.
76. G. B. McKenna, *J. Phys.: Condens. Matter*, 2003, **15**, S737.
77. H. E. H. Meijer, L. E. Govaert, *Prog. Polym. Sci.*, 2005, **30**, 915.
78. L. C. E. Struik, *Physical Aging in Amorphous Glassy Polymers and Other Materials*, Elsevier, Amsterdam, 1978.
79. D. Cangialosi, M. Wübbenhorst, H. Schut, S. Picken, *Acta Phys. Pol. A*, 2005, **107**, 690.
80. K. Hebert, M. D. Ediger, *Macromolecules*, 2017, **50**, 1016.
81. S. L. Bazhenov, Yu. A. Rodionova, A. S. Kechekyan, *Polym. Sci.*, *Ser. A* (*Engl. Transl.*), 2005, **47**, 126.
82. A. L. Volynskii, N. F. Bakeev, *Solvent Crazing of Polymers*, Elsevier, Amsterdam, New-York, 1995, 423 c.
83. A. L. Volynskii, N. F. Bakeev, *Strukturnaya samoorganizatsiya amorfnykh polimerov* [*Structural Self-organization of Polymers*], Fizmatlit, Moscow, 2005, 230 pp. (in Russian).
84. R. P. Kambour, *J. Polym. Sci.*, *Macromol. Rev.*, 1973, **7**, 1.
85. A. M. Donald, *Crazing*, in *The Physics of Glassy Polymers*, Ed. R. N. Haward, R. J. Young, Springer Netherlands, Dordrecht, 1997, 295—341.
86. E. Passaglia, *J. Phys. Chem. Solids*, 1987, **48**, 1075.
87. G. Taylor, *Proc. R. Soc. Lond. A*, 1950, **201**, 192.
88. E. J. Kramer, *Microscopic and Molecular Fundamentals of Crazing*, in *Crazing in Polymers*, Ed. H. H. Kausch, Springer, Berlin, Heidelberg, 1983, **52/53**, 1—56.
89. E. Paredes, E. W. Fischer, *Macromol. Chem.*, 1979, **180**, 2707.
90. A. V. Efimov, V. Yu. Shcherba, A. V. Rebrov, A. N. Ozerin, N. F. Bakeyev, *Polym. Sci. USSR* (*Engl. Transl.*), 1990, **32**, 400.
91. A. V. Efimov, V. Yu. Shcherba, A. V. Rebrov, A. N. Ozerin, N. F. Bakeyev, *Polym. Sci. USSR* (*Engl. Transl.*), 1990, **32**, 769.
92. A. V. Efimov, V. Yu. Shcherba, N. F. Bakeyev, *Polym. Sci. USSR* (*Engl. Transl.*), 1989, **31**, 2569.
93. A. N. Gent, *J. Macromol. Sci.*, *Part B: Phys.*, 1973, **8**, 597.
94. V. A. Kargin, G. L. Slonimskii, *Kratkie ocherki po fizikokhimii polimerov* [*Short Essays on Physical Chemistry of Polymers*], Khimiya, Moscow, 1967, 232 pp. (in Russian).
95. Yu. A. Shlyapnikov, *Russ. Chem. Rev.* 1997, **66**, 963.
96. V. N. Belousov, G. V. Kozlov, A. L. Mikitaev, Yu. S. Lipatov, *Dokl. Chem.* (*Engl. Transl.*), 1990, **313**.
97. L. Bove, C. D´Aniello, G. Gorrasi, L. Guadagno, V. Vittoria, *Polym. Bull.*, 1997, **38**, 579.
98. F. J. B. Calleja, C. S. Cruz, T. Asano, *J. Polym. Sci.*, *Part B: Polym. Phys.*, 1993, **31**, 557.
99. V. Vittoria, E. Petrillo, R. Russo, *J. Macromol. Sci.*, *Part B: Phys.*, 1996, **35**, 147.
100. K. Neki, P. H. Geil, *J. Macromol. Sci.*, *Part B: Phys.*, 1973, **8**, 295.
101. S. Venkatesan, S. Basu, *J. Mech. Phys. Solids*, 2015, **77**, 123.
102. P. B. Bowden, S. Raha, *Phil. Mag.*, 1970, **22**, 463.
103. I. M. Ward, *Polym. Eng. Sci.*, 1984, **24**, 724.
104. J. C. M. Li, *Polym. Eng. Sci.*, 1984, **24**, 750.
105. J. P. Harmon, S. Lee, J. C. M. Li, *Polymer*, 1988, **29**, 1221.
106. A. L. Volynskii, L. M. Yarysheva, A. A. Mironova, O. V. Arzhakova, A. S. Kechekyan, A. N. Ozerin, A. V. Rebrov, N. F. Bakeev, *Polym. Sci.*, *Ser. A* (*Engl. Transl.*), 1996, **38**, 152.
107. A. L. Volynskii, L. M. Yarysheva, O. V. Arzhakova, N. F. Bakeev, *Polym. Sci. USSR.* (*Engl. Transl.*), 1991, **33**, 344.
108. K. Friedrich, in *Crazing in Polymers*, Ed. H. H. Kausch, Springer, Berlin, Heidelberg, 1983, **52/53**, p. 225.
109. Yu. S. Lazurkin, Thesis. Doctor of Phys.-Math. Sciences, Institute of Physical Problems, RAS, Moscow, 1954.
110. L. A. Laius, E. V. Kuvshinskii, *Polym. Sci. USSR* (*Engl. Transl.*), 1964, **6**, 60.
111. V. I. Shoshina, G. V. Nikonovich, Yu. T. Tashpulatov, *Izometricheskii metod issledovaniya polimernykh materialov* [*Isometric Method for Studying Polymeric Materials*], Izd. AN Uzb. SSR, Tashkent, 173 pp. (in Russian).
112. S. A. Arzhakov, Thesis, Doctor of Chemical Sciences, NIFKHI L.Ya. Karpov, Moscow, 1975.
113. E. F. Oleynik, in *High Performance Polymers*, Ed. E. Baer, S. Moet, Hauser Verlag, Berlin, 1991, p. 79.
114. E. F. Oleinik, O. B. Salamatina, S. N. Rudnev, S. V. Shenogin. *Polym. Sci.*, *Ser. A* (*Engl. Transl.*), 1993, **35**, 1532].

115. S. V. Shenogin, G. W. H. Hohne, O. B. Salamatina, S. N. Rudnev, E. F. Oleinik, *Polym. Sci.*, *Ser. A* (*Engl. Transl.*), 2004, **46**, 21.
116. M. Trznadel, T. Pakuia, M. Kryszewski, *Polymer*, 1988, **29**, 619.
117. H. W. Starkweather Jr, *Polymer*, 1991, **32**, 2443.
118. C. Zhang, Y. Guo, R. D. Priestley, *J. Polym. Sci.*, *Part B: Polym. Phys.*, 2013, **51**, 574.
119. S. Feng, Y. Chen, B. Mai, W. Wei, C. Zheng, Q. Wu, G. Liang, H. Gao, F. Zhu, *Phys. Chem. Chem. Phys.*, 2014, **16**, 15941.
120. J. A. Forrest, K. Dalnoki-Veress, *Adv. Colloid Interface Sci.*, 2001, **94**, 167.
121. R. Huang, C. Stafford, B. Vogt, *J. Aerosp. Eng.*, 2007, **20**, 38.
122. C. S. Stevenson, J. G. Curro, J. D. McCoy, *J. Chem. Phys.*, 2017, **146**, 203322.
123. H. W. Cho, B. J. Sung, *Soft Matter*, 2017, **13**, 1190.

Received July 10, 2017;
in revised form November 20, 2017;
accepted November 25, 2017